

Persistence of a reef fish metapopulation via network connectivity: theory and data

Allison G. Dedrick^{a,*}

Katrina A. Catalano^a

Michelle R. Stuart^a

J. Wilson White^b

Humberto Montes, Jr.^c

Malin Pinsky^a

a. Department of Ecology Evolution and Natural Resources, Rutgers University, 14
College Farm Road, New Brunswick, NJ 08901 USA;

b. Department of Fisheries and Wildlife, Coastal Oregon Marine Experiment Sta-
tion, Oregon State University, Newport, OR 97365 USA;

c. Visayas State University

* Corresponding author; e-mail: agdedrick@gmail.com

(Author order not yet determined)

Introduction

Metapopulation dynamics and persistence depend on connectivity among patches
3 and the demographic rates at each patch (e.g. Hastings and Botsford, 2006; Hanski,
1998). Assessing levels of connectivity and demographic parameters has been par-
ticularly challenging for marine species, where much of the mortality and movement
6 happens at larval and juvenile stages when individuals are hard to track and have
the potential to travel long distances with ocean currents (reviewed in White et al.,
2019). A need to understand metapopulations for conservation and management,
9 such as siting marine protected areas (e.g. Botsford et al., 2001; White et al., 2010),
however, has led to a large body of theory describing how marine metapopulations
might persist.

12 For any population to persist, individuals must on average replace themselves
during their lifetime. Assessing replacement must take into account the demographic
processes across the whole life cycle, including how likely individuals are to survive to
15 the next age or stage, their expected fecundity at each stage, and the survival of any
offspring produced to recruitment. In a spatially structured population, as many
marine populations are, in addition to assessing whether the reproductive output
18 and survival of a population is sufficient, we must also consider how the offspring are
distributed across space.

Considering both the demographic processes within patches and the connectivity
21 among them, a metapopulation can persist in two ways: 1) at least one patch can
achieve replacement in isolation, or 2) patches receive enough recruitment to achieve

replacement through multi-generational loops of connectivity with other patches in
24 the metapopulation (Hastings and Botsford, 2006; Burgess et al., 2014). In the first
case (termed self-persistence), enough of the reproductive output produced at one
patch is retained at the patch for it to persist. In the second (network persistence),
27 closed loops of connectivity among at least some of the patches - where individuals
from one patch settle at another and eventually send offspring back to the first in a
future generation - provide the patch with enough recruitment to persist within the
30 network. Though it has been challenging to estimate the parameters necessary to
understand how actual metapopulations persist, a large work of theory developed in
part to guide marine protected area design helps predict when each type of persistence
33 is likely to occur (i.e., habitat patches or protected areas that are large relative to
the mean dispersal distance are likely to be self-persistent, White et al., 2010).

New ways of identifying individuals and determining their origins, such as otolith
36 and shell microchemistry and genetic parentage analysis (e.g. Wang, 2004, 2014), now
allow us to better measure dispersal (e.g. Almany et al., 2017; D'Aloia et al., 2013)
and a better appreciation of the relevant population dynamic theory has led to mea-
39 surement of the appropriate demographic factors (e.g. Carson et al., 2011; Hameed
et al., 2016) necessary to assess persistence in real metapopulations. We might ex-
pect that populations on isolated islands are the most likely to be self-persistent, as
42 they lack nearby populations with which to exchange larvae and would go locally
extinct if they did not achieve replacement. At isolated Kimbe Island in Papua New
Guinea, Salles et al. (2015) find that the population of orange clownfish (*Amphiprion*
45 *percula*) can likely persist without outside immigration. In contrast, populations of

bicolor damselfish (*Stegastes partitus*) at four study sites nested within a larger reef metapopulation in the Bahamas do not appear able to persist without outside input
48 (Johnson et al., 2018). Persistence has yet to be assessed in the field for an entire marine metapopulation, such as all of the patches in a coastal metapopulation.

The number of studies estimating demographic rates and connectivity in marine
51 metapopulations is growing (e.g. Carson et al., 2011; Salles et al., 2015; Johnson et al., 2018; Garavelli et al., 2018), but most use data from one or a few years. Longer data sets enable better estimates of long-term average rates, rather than
54 assuming the demographic and dispersal rates from a particular year or two are representative. Long data set are also useful for explicitly considering uncertainty, both to assess how well we understand persistence for a population and to assess
57 which parameters contribute most to our uncertainty. Finally, sampling over many years provides abundance trends to compare with persistence metrics.

Here, we further our understanding of metapopulation dynamics in a network
60 of patches along a coastline through a study of yellowtail clownfish (*Amphiprion clarkii*) in the Philippines. We assess persistence for all patches of habitat within a 30 km stretch of coastline, exceeding estimates of the dispersal spread for this species
63 (Pinsky et al., 2010), suggesting the network is likely to operate as a contained metapopulation. With seven years of annual sampling data, we are able to estimate persistence metrics and replacement over the longer term and investigate abundance
66 through time to compare with the replacement-based persistence metrics. We use our long-term data set from habitat patches on a continuous section of coastline to understand persistence within a local network. We find that our sites have stable

⁶⁹ abundances through time but are unlikely to persist as an isolated metapopulation
and require immigration from outside patches to persist.

Methods

⁷² Persistence theory and metrics

For a population to persist, each individual must on average replace itself (e.g. Hastings and Botsford, 2006; Botsford et al., 2019). In non-spatially structured populations, we use criteria such as the average number of recruiting offspring each individual produces during its life (called R_0 when the population is age-structured and density-independent) or the growth rate of the population (such as the dominant eigenvalue λ of an age-structured Leslie matrix) (Caswell, 2001; Burgess et al., 2014). For spatially-structured populations, we must also consider the spatial spread of offspring, often represented through a dispersal kernel or connectivity matrix (Burgess et al., 2014).

We consider four primary metrics to assess whether and how the population is persistent: 1) lifetime recruit production (LRP), to assess whether the population has enough surviving offspring to achieve replacement, 2) self-persistence (SP), to assess whether any individual patch can persist in isolation without input from other patches, 3) network persistence (NP), to assess whether the metapopulation is persistent as a connected unit, and 4) local replacement (LR), as second assessment of whether individuals replace themselves with recruits retained within population. We explain each metric below in detail. To represent the uncertainty in our estimates, we

⁹⁰ calculate each metric 1000 times, sampling each input parameter from a distribution
that represents the uncertainty in each empirical estimate of demographic rates or
connectivity. In our results, we show our best estimate of each persistence metric
⁹³ along with the range of uncertainty values.

Lifetime recruit production

We find the estimated number of recruits an individual recruit will produce (lifetime
⁹⁶ recruit production: LRP) by multiplying the total number of eggs a recruit-sized
individual will produce in its lifetime (lifetime egg production: LEP) by the fraction
of those eggs that will survive to become recruits (egg-recruit survival: S_e) (Fig. 1):

$$\text{LRP} = \text{LEP} * S_e. \quad (1)$$

⁹⁹ If $\text{LRP} \geq 1$, the population has the potential for replacement; individuals produce
enough surviving offspring, before considering dispersal. If $\text{LRP} < 1$, the individuals
are not replacing themselves and the population cannot persist without input from
¹⁰² outside patches and is a sink habitat within a larger metapopulation (Pulliam, 1988).
We use all recruits produced by adults in our population to estimate LRP , regardless
of where they settle.

¹⁰⁵ Self-persistence

A patch is able to persist in isolation (self-persistent) if individuals produce enough
offspring that survive to recruitment (LRP) and settle in the natal patch (i , with

¹⁰⁸ probability of dispersal $p_{i,i}$) to replace themselves:

$$SP_i = \text{LRP}_i \times p_{i,i}. \quad (2)$$

A patch i is self-persistent if $SP_i \geq 1$. If at least one patch is self-persistent, the metapopulation as a whole is persistent as well (Hastings and Botsford, 2006; ¹¹¹ Burgess et al., 2014). Our equation for SP is a modification of that used in Burgess et al. (2014), which uses LEP to represent offspring produced and uses local retention (the number of surviving recruits that disperse back to the natal patch divided by ¹¹⁴ the number of eggs produced by the natal patch) to capture egg-recruit survival and dispersal combined: $\text{LEP} \times \text{local retention} \geq 1$. We modify this to include egg-recruit survival in the offspring term instead, using LRP in place of LEP.

¹¹⁷ **Network persistence**

Network persistence explicitly considers dispersal of individuals among sites, a critical part of the larval life stage, in addition to the reproduction and survival at each ¹²⁰ site. We represent dispersal with a dispersal kernel, which relates the likelihood of an individual dispersing to the distance traveled. We find the probabilities of a recruit dispersing between each set of sites ($p_{i,j}$) by integrating the dispersal kernel ¹²³ over the distances between sites. We then create a realized connectivity matrix C by multiplying the dispersal probabilities by the expected number of recruits an individual produces: $C_{i,j} = \text{LRP} \times p_{i,j}$ (Burgess et al., 2014, though we include egg-

¹²⁶ recruit survival in LRP, rather than in $p_{i,j}$ as they do). The diagonal entries of C , where the origin and destination are the same site, are the values of self-persistence for each individual site.

¹²⁹ Network persistence evaluates the largest real eigenvalue of the realized connectivity matrix λ_C , which must be greater than 1 for the network to persist without outside input: $NP = \lambda_C \geq 1$ (e.g. Hastings and Botsford, 2006; White et al., 2010; ¹³² Burgess et al., 2014).

Local replacement

Like network persistence, local replacement (LR) assesses whether the population ¹³⁵ is locally self-sustaining. Rather than considering dispersal explicitly as network persistence does, local replacement modifies LRP to estimate the average number of recruits produced per individual that return to settle within our sites. We estimate ¹³⁸ LR by multiplying LEP by the proportion of eggs produced that survive and return to recruit at our sites (R_e), a modification of egg-recruit survival that implicitly includes dispersal. If $LR \geq 1$, individuals produce enough locally-retained offspring ¹⁴¹ to replace themselves and the population can persist in isolation.

$$LR = LEP \times R_e. \quad (3)$$

Study system

We focus on a tropical metapopulation of yellowtail clownfish (*Ampiprion clarkii*, Fig. ¹⁴⁴ 2c) on the west coast of Leyte island facing the Camotes Sea in the Philippines (Fig.

2a). Like many clownfish species, yellowtail clownfish have a mutualistic relationship with anemones that house small colonies of fish (Buston, 2003b; Fautin et al., 1992).

147 Yellowtail clownfish are protandrous hermaphrodites and maintain a size-structured hierarchy; within an anemone, the largest fish is the breeding female, the next largest is the breeding male, and any smaller fish are non-breeding juveniles. The fish
150 move up in rank to become breeders only after the larger fish have died. In the tropical patch reef habitat of the Philippines, yellowtail clownfish primarily spawn from November to May, laying clutches of benthic eggs that the parents protect and
153 tend (Ochi, 1989; Holtswarth et al., 2017). Larvae hatch after about six days and spend 7-10 days in the water column before returning to reef habitat to settle in an anemone (Fautin et al., 1992).

156 Clownfish are particularly well-suited to metapopulation studies due to their limited movement as adults and well-defined patchy habitat. Once fish have settled, they tend to stay within close proximity of their anemones, which are found on reef
159 patches. This makes fish easier to relocate for mark-recapture studies and simplifies the exchange between patches to only dispersal during the larval phase. Patches, whether considered to be the reef patch or the anemone territory of the fish, are
162 discrete and easily delineated (Fig. 2a, b), which makes determining the spatial structure of the metapopulation clear. Additionally, clear patches make it easier to assess how much of the site has been surveyed. These simplifying characteristics in habitat and fish behavior make clownfish and other similarly territorial reef
165 fish useful model systems for studies of metapopulation dynamics and persistence (e.g. Buston and DAloia, 2013; Salles et al., 2015; Johnson et al., 2018). Our fo-

¹⁶⁸ cal species of yellowtail clownfish tends to behave more like larger reef fishes, with
wider-ranging territories and stronger swimming abilities (Hattori and Yanagisawa,
1991; Ochi, 1989), than the smaller clownfish *A. percula* commonly used in previous
¹⁷¹ metapopulation studies (e.g. Buston et al., 2011; Salles et al., 2015). As we show
later, survival in yellowtail clownfish is also lower than *A. percula* and more similar
to other damselfishes. MAKE SURE THIS SENTENCE IS TRUE!

¹⁷⁴ **Field data collection**

We focus on a set of nineteen patch reef sites spanning 30 km along the western coast
of Leyte island (Fig. 2a). The sites consist of rocky patches of coral reef separated
¹⁷⁷ by sand flats, with reef patches covering approximately 20% of the sampling region
(Fig. 2b). On the north edge, the sites are isolated from nearby habitat with no
substantial reef habitat for at least 20 km.

¹⁸⁰ Since 2012, we have sampled fish and habitat at most of the sites annually (Table
A2). During sampling, divers using SCUBA and tethered to GPS readers swam the
extent of each site. Divers visited each anemone inhabited by yellowtail clownfish
¹⁸³ and tagged anemones. At each anemone, the divers attempted to catch all of the
yellowtail clownfish 3.5 cm and larger, took a small tail fin-clip from each for use in
genetic analysis, measured the fork length, and noted the tail color (as an indicator of
¹⁸⁶ life stage). Starting in the 2015 field season, fish 6.0 cm and larger were also tagged
with a passive integrated transponder (PIT) tag, unless already tagged. Divers also
looked for eggs around each anemone and measured and photographed any clutches
¹⁸⁹ found. In total, we took fin clips from and genotyped 2407 fish and PIT-tagged 1930

fish across all years and sites combined, marking 3053 individual fish.

192 Estimating demographic and dispersal parameters from empirical data

Parentage analysis and dispersal kernel

Over seven years of sampling, we genotyped 1719 potential parents and 785 juveniles
195 and found 62 parent-offspring matches (details in Catalano et al., in prep). We use a distance-based dispersal kernel fit from the parent-offspring matches (Catalano et al.,
in prep), where the relative dispersal $p(d)$ is a function of distance d in kilometers and
198 parameters $\theta = 1.19$ and $z = e^{k_d=-2.33}$ that control the shape and scale of the kernel:
 $p(d) = ze^{-(zd)^\theta}$. The dispersal kernel estimates the relative dispersal by distance for fish that have survived and recruited so does not estimate pre-settlement mortality.
201 To find the probability of fish dispersing among our sites, we numerically integrate the dispersal kernel using the distance from the middle of the origin site (i) to the closest (d_1) and farthest (d_2) bounds of the destination site (j):

$$p_{i,j}(d) = \int_{d_1}^{d_2} ze^{-(zd)^\theta} dd. \quad (4)$$

204 To account for uncertainty in the dispersal kernel, we use sets of the shape parameter θ and the scale parameter k_d that represent the span of the 95% confidence interval when k_d and θ are estimated jointly (Catalano et al., in prep).

207 **Growth and survival: mark-recapture analyses**

We marked fish with both genetic samples and PIT tags, allowing us to estimate growth and survival through mark-recapture. In total, we have 3053 marked fish
210 with size and stage data for each capture time.

For growth, we estimated the parameters of a von Bertalanffy growth curve (Fabens, 1965) in the growth increment form relating the length at first capture
213 L_t to the length at a later capture L_{t+1} (Hart and Chute, 2009), where L_∞ is the average asymptotic size across the population and K controls the rate of growth:

$$\begin{aligned} L_{t+1} &= L_t + (L_\infty - L_t)[1 - e^{(-K)}] \\ &= e^{(-K)}L_t + L_\infty[1 - e^{(-K)}]. \end{aligned} \tag{5}$$

We see from eqn. 5 that we would expect the first length L_t and the second length
216 L_{t+1} to be related linearly (Hart and Chute, 2009). From the slope $m = e^{(-K)}$ and y-intercept $b = L_\infty[1 - e^{(-K)}]$, we calculated the von Bertalanffy parameters, such that $K = -\ln m$ and $L_\infty = \frac{b}{(1-m)}$. We used the first and second capture lengths
219 for fish that were recaptured after a year (within 345 to 385 days) to estimate L_∞ and K . We have some fish that were recaptured more than two times so we randomly selected only one pair of recaptures from each to use to estimate the parameters
222 1000 times. We found the mean estimates and mean standard error of those fits, then sampled from within than range to generate a set of von Bertalanffy growth curves to use in our metric uncertainty calculations.

225 We used the full set of marked fish to estimate annual survival ϕ and probability of
recapture p_r using the mark-recapture program MARK implemented in R through
the package **RMark** (Laake, 2013). We fit several models with year, size, and site
228 effects on the probability of survival on a log-odds scale (see full list in Table A4).
For fish that were not recaptured in a particular year, we estimated their size using
our growth model (eqn. 5) and the size recorded or estimated in the previous year.
231 Fish are not well-mixed at our sites and divers needed to swim near an anemone to
have a reasonable chance of capturing the fish on it so we also considered a distance
effect on recapture probability. Using diver GPS tracks, we estimated the minimum
234 distance between a diver and the anemone for each tagged fish in each sample year
to include as a factor. We compared the fit of the models using a modified version of
the Akaike information criterion that reduces the potential for overfitting with small
237 sample sizes (AICc) and selected the model with the lowest AICc value. (Table A4).

Fecundity

We used a size-dependent fecundity relationship determined using photos of egg
240 clutches and females (Yawdoszyn, in prep), where the number of eggs per clutch
(E_c) is exponentially related to the length in cm of the female (L) with size effect
 $\beta_l = 2.388$, intercept $b = 1.174$, and egg age effect $\beta_e = -0.608$ dependent on if the
243 eggs are old enough to have visible eyes. We multiplied the number of eyed eggs per
clutch by the number of clutches per year $c_e = 11.9$ (estimate from Holtswarth et al.,
2017) to get total annual fecundity f of a female of length L :

$$f = c_e * e^{\beta_l \ln(L) + \beta_e [\text{eyed}] + b}. \quad (6)$$

²⁴⁶ **Lifetime egg production**

We used an integral projection model (IPM) (Ellner et al., 2016) with size as the continuous structuring trait z to estimate lifetime egg production (LEP), the expected total number of eggs produced by one recruit. We initialized the IPM with one recruit-sized individual at the initial annual time step ($t = 0$), then projected forward for 100 time steps. We used the size-dependent survival (eqn. B.5) and growth (eqn. 5) functions as the probability density functions in the kernel to describe the survival and growth of the individual into the next time step. We get the size distribution (v_z) at each time step, which represents the probability that the individual has survived and grown into each of the possible size categories, ranging from a minimum of $L_s = 0$ cm to a maximum of $U_s = 15$ cm divided into 100 equal size bins. The probability that the individual is still alive and of any size decreases as the time steps progress; by using a large number of steps, we are able to avoid arbitrarily setting a maximum age and instead let the probabilities become essentially zero.

²⁶¹ We then multiplied the size-distribution v_z at each time by the size-dependent fecundity f_z described above (eqn. 6) to get the total number of eggs produced at each time step. Integrating across time and size gives the total number of eggs one individual is likely to produce in its lifetime:

$$\text{LEP} = \int_{t=0}^{100} \int_{z=L_s}^{z=U_s} v_{z,t} f_z dz dt. \quad (7)$$

When entering the starting individual into the matrix, we use 0.1 as the standard deviation of size to spread the starting individual across size bins. When projecting the distribution of the size of the fish in the next year, we used the size determined by the growth curve (eqn. 5) as the mean along with an estimate of spread to account for differences in fish growth rates. We used our recapture data to estimate the standard deviation (size_{sd}) of the distribution of sizes in the next year of fish starting from one size (A1).

We only considered reproductive effort once the fish has reached the female stage and use the average size of first observation as female for recaptured fish as the transition size $L_f = 9.32\text{cm}$. To incorporate uncertainty, we sampled directly from the sizes at which recaptured fish were first captured as female (5.2 cm - 12.7 cm) (Fig. 3d).

Survival from egg to recruit

We estimate survival from egg to recruit (S_e) using parentage matches to find the number of surviving recruits produced by genotyped parents (similar to the method in Johnson et al., 2018). We scale the number offspring we assign back to parents ($R_m = 62$) by various ways we could have missed offspring in our sampling (P_h , P_c , P_d , and P_s , described below and in Fig. B.1), then divide by the estimated number of eggs produced by genotyped parents (the number of genotyped parents $N_g = 1719$

multiplied by the expected LEP for a fish of parent size LEP_p ;)

$$S_e = \frac{\frac{R_m}{P_h P_c P_d P_s}}{N_g \text{LEP}_p}. \quad (8)$$

We scale the number of matched recruits we find by the cumulative proportion of habitat in our sites we sampled over time ($P_h = 0.41$, details in B.1), the probability of capturing a fish if we sampled its anemone ($P_c = 0.56$, see B.2 for details), and the proportion of the total dispersal kernel area from each of our sites covered within our sampling region ($P_d = 0.28$, calculation in B.3.0.1). Finally, because our dispersal kernel gives the probability of dispersal given that a recruit settled somewhere but our sampling region is not all habitat, we scale by the proportion habitat in our sampling region ($P_s = 0.20$, details in B.3.0.2) to avoid counting this mortality twice.

To estimate local replacement, we scale only by the proportion of habitat we cumulatively sample in our sites and the probability of capturing a fish to estimate the survival and retention of recruits back to our sites: $R_e = \frac{\frac{R_m}{P_h P_c}}{N_g \text{LEP}_p}$.

To incorporate uncertainty in our estimate of egg-recruit survival, we consider uncertainty in the number of offspring assigned to parents during the parentage analysis (R_m) and in the probability of capturing a fish (P_c). We generate a set of values for the number of assigned offspring using a random binomial, where the number of trials is the number of genotyped offspring (745) and the probability of success on each trial is the assignment rate of offspring from the parentage analysis (0.079) (Catalano et al., in prep). For the probability of capturing a fish, we sample values from a beta distribution that captures the mean and variance of capture

probabilities across recapture dives (details in B.2).

Defining recruit and census stage

When assessing persistence, it is important to consider mortality and reproduction that occurs across the entire life cycle to determine whether an individual is replacing itself with an individual that reaches the same life stage (Burgess et al., 2014). We define a recruit to be a juvenile individual that has settled on the reef within the previous year, which also encompasses the size we are first able to sample (3.5-6.0 cm for parentage studies) (Fig. 1). In theory, it does not matter how we define a recruit as long as we use that definition in our calculations of both egg-recruit survival and LEP. In our system, however, while it is straightforward to calculate LEP from any size, we did not have enough tagged recruits to reliably estimate survival to different recruit sizes. Instead, we choose the mean size of offspring matched in the parentage study as our best estimate of the size of a recruit ($\text{size}_{\text{recruit}}$) and test sensitivity to different recruit sizes by sampling from a uniform distribution over the sizes the recruit stage covers (3.5-6 cm, Table A1).

Accounting for density-dependence

Ideally we would assess persistence metrics when the population is at low abundance and not limited by density-dependence. Clownfish have strong social hierarchies and juveniles on an anemone will prevent others from settling there as well (seen in *A. percula*, Buston, 2003a). Each anenome, therefore, can house only one settling clownfish, with anemones already occupied by *A. clarkii* settlers essentially unavail-

able as habitat. This density-dependent mortality will artificially reduce the apparent survival of new recruits, biasing persistence metrics. We account for this density-
 327 dependent mortality by multiplying our estimate of settling recruits (the numerator of eqn. 8) by the proportional increase (DD) in unoccupied anemones at our sites if all of the *A. clarkii* anemones were unoccupied, where p_A is the proportion of
 330 anemones occupied by *A. clarkii* and p_U is the proportion of unoccupied anemones:

$$\text{DD} = \frac{(p_U + p_A)}{p_U} = 1.71.$$
 We present results with this density-dependence modification (with subscript DD: LRP_{DD} in the main text and without in the appendix (Figs.
 333 C.2, C.3)).

Estimated abundance over time

We also consider trends in abundance of breeding females at each site over time ($F_{i,t}$)
 336 to compare to our replacement-based estimates of persistence. Similarly to as we do for offspring, we scale up the number of females caught (F_c) at each site i in each sampling year t by the proportion of habitat sampled in that site and year $P_{h_{i,t}}$ and
 339 by the probability of capturing a fish P_c :

$$F_{i,t} = \frac{F_{c_{i,t}}}{P_{h_{i,t}} P_c} \quad (9)$$

We fit a mixed effects model to estimate the number of fish in each year as a Poisson variable λ_a with site as a random effect m_i using the package `lme4` in R

³⁴² (Bates et al., 2015):

$$\begin{aligned} F_{i,0} &\sim Poisson(\lambda_a) \\ F_{i,t} &= (\lambda_a + m_i)^t. \end{aligned} \tag{10}$$

We estimate λ_a for an average site as well as the individual sites. The population is increasing over time if $\lambda_a > 1$ and decreasing if $\lambda_a < 1$.

(11)

³⁴⁵ Results

From the mark-recapture analysis of tagged and genotyped fish, we estimated mean values of $L_\infty = 10.70$ cm with 95% confidence intervals 9.81-11.65 and $K = 0.864$ ³⁴⁸ (0.80-0.91) for the von Bertalanffy growth curve parameters (eqn. 5, Fig. 3b, Table A1). For juvenile and adult (post-recruitment) survival on a log-odds scale, the best-fit model has an effect of site and a positive effect of size (eqn. B.5, Table A1, Figs. ³⁵¹ 3c, B.3). The accompanying best-fit model for recapture probability has negative effects of size and diver distance from anemone (eqn. B.6, Table A1, Fig. B.4).

For our persistence metrics, we present the estimate using the input values without considering uncertainty (the mean of the uncertainty distributions, with the exception of the size range for recruit), as the best estimate and the range with uncertainty shown in brackets. Using our best estimates for growth, survival, and fecundity, we calculated an average value of LEP across sites of 721 eggs [82, 31657] ³⁵⁷

(Fig. 4b), with best estimates at individual sites ranging from 0 to 1754 eggs (Fig. C.4). Adult survival has the most effect on the value of LEP (Fig. C.7), with LEP higher the higher the annual survival of adults, who then have more opportunities to reproduce and produce more eggs per clutch when they are larger.

We estimated egg-recruit survival $S_{e_{DD}}$ to be 0.002 [3.5e-05, 0.014] when we correct for density-dependence in our data. Uncertainty in the size of transition to breeding female L_f has the largest effect on egg-recruit survival (Fig. C.9); the larger the transition size to female, the fewer tagged eggs we estimate were produced by our genotyped parents and the higher our estimate of egg-recruit survival. This differs from our finding above that adult survival has the largest effect on LEP because the starting size of the individual considered is lower when we estimate LEP for a recruit (4.37 cm, 3.5-6.0cm range) than LEP for a parent (6.0cm). Fish considered as parents in our parentage analysis have already survived one or more years since recruiting so the transition to breeding female plays a larger role in the number of eggs they are likely to produce than for fish who have just recruited.

We estimated average lifetime recruit production (LRP_{DD}) across sites, the product of LEP_i and $S_{e_{DD}}$, to be 1.45 [0.62, 7.78] (Fig. 4c). Our best estimates of LRP_{DD} at individual sites range from 0 to 3.5 (Fig. C.5). 94% of the estimates of LRP with density-dependence compensation and the average best estimate across sites are one or greater, above the threshold necessary for replacement before considering dispersal. This means that individuals at our sites produce enough surviving offspring before considering dispersal to be able to replace themselves, but LRP does not tell us whether those offspring will settle within our sample sites and drive persistence.

381 We did not find any sites with a best estimate of $SP_{DD} \geq 1$ (Fig. 5a), suggesting
382 that none of our sites could persist in isolation. The site Haina ($SP_{DD} = 0.047$ [9.5e-
383 05, 0.60]) has the largest SP but none of the estimates with uncertainty are ≥ 1 . We
384 saw estimates > 1 for Caridad Cemetery but those were due to the lack of recaptures
at that site and the resulting high uncertainty in adult survival and are unlikely to
indicate persistence.

387 Most of the connectivity occurs among the sites in the northern part of our
sample area, from Palanas to Caridad Cemetery, and at the southern part of our
sample area from Tomakin Dako to Sitio Baybayon (Fig. 5b), where the sites tend
390 to be the largest, have higher abundances, and have higher survivals (though not
entirely). Sites at the edges of our sampling region seem to be the strongest sub-
populations, which means many of the recruits they produce could be exported away
393 from our sites rather than into our sampling region.

For network persistence, our best estimate of the dominant eigenvalue of the
realized connectivity matrix $\lambda_{c_{DD}}$ is 0.15 [0.064, 1.54], $p(\lambda_{c_{DD}} \geq 1) = 0.005$ when we
396 correct for density-dependence in the data (Fig. 5c). Network persistence for our
sites is unlikely but not impossible. Our estimate of local replacement (LR_{DD}) was
0.16 [0.07, 0.88] when correcting for density-dependence in the data, also suggesting
399 lack of independent persistence of our group of sites and very similar to our $\lambda_{c_{DD}}$
estimate. When we calculated LR using all arriving recruits to our sites, however,
rather than just those originating there, our best estimate was > 1 (2.08 with 99.8%
402 ± 1), suggesting that there is recruit-recruit replacement at our sites when we include
immigrant recruits. While both LR_{DD} and $\lambda_{c_{DD}}$ tell us about the ability of our sites

to persist as an isolated group, they differ in their assumption of the structure of the
405 population. LR_{DD} gives us the number of recruits individuals at our sites produce
that settle within our sites, assuming the network of sites is a single well-mixed unit,
while $\lambda_{c_{DD}}$ accounts for the spatial structure and multi-generation dynamics.

408 Based on our estimates of LRP_{DD} , LR_{DD} , SP_{DD} , and NP_{DD} , it is possible but
unlikely that our set of sets is able to persist in isolation as a closed system. With
our existing site configuration and dispersal kernel estimate, we would need a value
411 of LRP of 8.84 (an egg-recruit survival of 0.012 with our estimated value of LEP or
a value of LEP of 4406 with our estimated value of $S_{e_{DD}}$) to have a best estimate
of $\lambda_{c_{DD}} = 1$ and network persistence. Retaining essentially all recruits produced
414 from our sites would enable our set of sites to persist, given that LRP is very likely
 ≥ 1 , but with our estimated dispersal kernel, increasing the amount of habitat in
our region (currently about 20%) even to 100% gives a best estimate $\lambda_{c_{DD}} = 0.95$,
417 with 59% of the estimates with uncertainty ≥ 1 (Fig. 6) suggesting persistence of
the region is possible but not certain.

Our estimated abundance of females over time has a slight positive trend for the
420 average site ($\lambda_a = 1.08$, Fig. 4a), suggesting a slight increase in population size for
the population overall through time. Most individual sites also show a slight positive
trend in female abundance through time, though one large site shows declines (Fig.
423 4a, Fig. C.1s).

Discussion

In this first assessment of demographic persistence of a coastal marine metapopulation,
426 we did not find strong evidence for either self-persistence of an individual patch or network persistence of the entire system as an isolated region. Self-persistence of one of the larger sites or network persistence of the group of sites is possible at the
429 upper end of our estimates with uncertainty, but neither is suggested by our best estimates or 87.5% of the estimate range. This inability to persist as an isolated region does not necessarily mean that the populations at our sites are declining,
432 however. Our assessments of population trends - both abundance over time and replacement of recruits when we include immigrants - find that the population levels at our sites are stable or increasing slightly. Taken together, our metrics suggest
435 that the sites in our region have stable populations on average but require input of immigrants to persist. The portion of coastline we sampled is likely a sink region of a larger metapopulation, given that there does not seem to be a long-term deline in
438 the population.

For our sites to be able to persist as a network on their own, either the number of surviving recruits produced by an average recruit (LRP) would need to be higher or
441 more recruits would need to be retained within the region. To see a best estimate of network persistence with our existing site configuration and estimated connectivity, LRP would need to be about three times higher than our best estimate, which is within
444 our range of uncertainty (top 6.9% of estimates) and similar to estimates of lifetime reproductive success that include dispersal to the natal reef in *A. percula* in Kimbe

Bay (Salles et al., 2020), suggesting it is not an unreasonable level of production.
447 Alternately, higher connectivity and retention of offspring among our sites could
lead to network persistence. Though lack of sufficient connectivity and retention is
thought to inhibit network persistence in other systems (e.g., a collection of reserves
450 for eastern oysters (*Crassostrea virginica*) in the Pamlico Sound in North Carolina;
Puckett and Eggleston, 2016), low production of surviving recruits due to poor habi-
tad quality seems the more likely explanation in our system. Our dispersal kernel is
453 comparable to those estimated for other species of reef fish, both similar in shape
(e.g., Harrison et al., 2012; DAloia et al., 2015) and with a mean dispersal distance
of a similar range to that estimated for *A. percula* in Kimbe Bay (13.3 and 18.9 km
456 compared to our estimate of 8.2 km; Almany et al., 2017), which has been found to
be persistent without input from outside reefs (Salles et al., 2015). Our sites have
generally low reef health, however, due to anthropogenic effects such as pollution
459 and silt from a nearby gravel mine, which affect habitat and reduce production (as
in other clownfish systems; Salles et al., 2020; Hayashi et al., 2019). Adult survival
was lower at the two sites just downstream of the gravel mine (N. and S. Magbangon
462 in Fig. B.3).

We do not find clear evidence for network persistence for our sites despite esti-
mates of the mean dispersal distance of *A. clarkii* from previous genetic work (11
465 km, Pinsky et al., 2010) and from our samples (8.2 km, Catalano et al., in prep)
that are well within the 30 km span of our sites. Though the length of our sam-
pling region is more than twice the mean dispersal distance, usually sufficient for
468 persistence of a population in an isolated reserve (e.g. Lockwood et al., 2002), our

sampling region contains only about 20% habitat, rather than a continuous stretch, which may be too low of habitat coverage to support network persistence. Our sensitivity test to proportion habitat suggests that about 2.75 times more habitat in our sampling region would give a best estimate with network persistence, with 50% of our estimates showing persistence ($\lambda_{C_{DD}} \geq 1$) at about 30% habitat. Our individual sites are likely too small to see self-persistence: the largest site, Haina, is only about 0.8km wide, about 10 times smaller than the mean dispersal distance. This is in contrast to the findings on reefs surrounding the isolated Kimbe Island, where the overall population of *A. percula* and several lagoon subpopulations of similar size as our sites were self-persistent (Salles et al., 2015). Our sites are in an area that was hit in 2013 by Typhoon Haiyan, one of the strongest typhoons ever to make landfall, so reef habitat has recently been destroyed in the area, including one of our northern sampling sites. The suggestion of a habitat shortage in our sampling region is partially dependent on our assumption that larvae land in non-habitat between patches and die. Larvae have some navigational and habitat-finding capabilities (e.g. Elliott et al., 1995; Fisher, 2005), so we could be underestimating their ability to find habitat in our calculations, which would decrease the amount of habitat required for network persistence.

We suggest that our region is a sink area of a larger metapopulation but the area required for the larger persistent metapopulation depends on the production and connectivity of outside patches. If surrounding patch populations have a similar LRP and level of connectivity as our sites, increasing the area of the network to include them also would not achieve network persistence. If nearby sites have higher

492 egg production or egg-recruit survival, however, it might not take much of an increase
in area considered to create a persistent network. Nearby reef sites such as Cuatro
Isla, with higher coral cover and less silt, could have higher survival of fish and be
495 contributing recruits to our sites.

An alternative to our sampled sites as a sink portion of a larger metapopulation
is that variability in demography or dispersal on a longer scale than our sampling
498 time could lead to persistence. For example, rockfish on the west coast of the United
States have highly variable and episodic recruitment, where successful recruitment
events occur on the decadal scale and sustain the population until the next strong
501 recruitment event (e.g., Tolimieri and Levin, 2005). Though perhaps not as extreme
as in the California Current system, ocean connectivity is still variable in the Coral
Triangle region surrounding our study sites, with estimates suggesting that 20 year
504 simulations are necessary to capture the full extent (Thompson et al., 2018). Our
study, though relatively long term, could have missed a particularly strong recruit-
ment event that would enable local persistence of the set of populations we sampled.

507 Though we estimate abundance trends and do not find overall declines, it is
possible we could have missed declines due to our sampling design. Our sampling
study was designed for mark-recapture analyses rather than a comprehensive habitat
510 or abundance estimate so we did not sample all areas of all sites each year. We scale
up the number of fish we caught to account for those we missed using the proportion
of metal-tagged anemones we visited, which assumes that all tagged anemones are
513 equally likely to be sampled. In reality, tags that no longer have anemones next to
them are likely harder to find and sample. If anemones are disappearing over time

at our sites, we might be overestimating the number of fish present and missing that
516 our site are declining and not persistent even with outside input.

NEED TO EDIT THIS UNCERTAINTY PARAGRAPH! Including uncertainty in our empirical estimates of demographic and dispersal parameters allows us to
519 better understand how likely it is that the population is persistent and which processes contribute the most uncertainty. We see a wide range of estimated metric values, spanning of network persistence for our set of sites to far from it. In our
522 study, demographic parameters, particularly adult survival, also have a large effect on whether or not we think the population is persistent. Other metapopulation studies also find higher sensitivity to demographic rather than connectivity parameters (e.g., on source or sink status in bicolor damselfish; Figueira, 2009), including particular sensitivity to adult survival (on metapopulation growth rate in mussels; Carson et al., 2011). Our estimates of connectivity are simpler than our estimates of
525 demography, with no spatial variability (which can be important in understanding demographic connectivity; Johnson et al., 2018), and a more thorough assessment could alter their relative effect on persistence, but this suggests that sufficient offspring production and survival has a larger effect on persistence at these relatively small scales of connectivity. Uncertainty in our sampling, particularly how likely we are to capture a fish, however, contributes the most uncertainty to whether we
531 determine the population to be persistent, highlighting the challenge of estimating these metrics empirically. For a marine metapopulation, our system is relatively uncomplicated; as we accumulate more empirical assessments of metapopulations to
534 compare to our expectations from theory and models, we will have to think carefully

about how to handle uncertainty as we move to tackling larger and more complicated systems.

540 Persistence criteria, such as those detailed in Hastings and Botsford (2006) and
Burgess et al. (2014), ask whether a population at low abundance can grow and
recover rather than going extinct. Density-dependence is often ignored at low abun-
543 dances (Botsford et al., 2019) so is not explicitly considered in persistence metrics.
In real populations, however, it can be challenging to estimate density-independent
demographic rates, as density-dependence is occurring in the population as it is
546 sampled. In *A. clarkii*, density-dependence is likely most important immediately
post-settlement, as for many fish species, but is also relatively easy to measure at
that point and accounted for in our analyses. Density-dependence could continue
549 to be important throughout the life history, however, due to the social hierarchies
in colonies of clownfish (e.g. Buston and Elith, 2011). In other species of clownfish,
individuals on the same anemone maintain strict size spacing, restricting their food
552 intake and growth to avoid encroaching on the position of another fish and being
attacked or evicted (seen in *A. percula*, Buston, 2003a,b). This suggests that while
fish are in the pre-reproductive queue, density-dependence may lower growth rates
555 compared to the growth of fish alone on an anemone, as would be the case in a pop-
ulation at low abundance. We include the primary effect of density-dependence on
our estimate of egg-recruit survival but other estimates, particularly growth and sur-
558 vival, would also likely be higher in the absence of density-dependence and increase
LRP.

Understanding persistence is critical for management of spatial-structured pop-

561 ulations, such as siting marine protected areas XX, assessing habitat fragmentation
562 risks, and conserving species in the face of climate change XX. Though models and
563 theory provide us with expectations, we are only recently beginning to be able to
564 tackle these questions of persistence empirically in model systems such as clownfish
565 and other sedentary tropical reef fish (e.g., Salles et al., 2015; Johnson et al., 2018).
566 With parentage analyses now being extended to temperate species (e.g., Baetscher
567 et al., 2019) and better understanding of how biophysical models compare to lar-
568 val dispersal patterns (Bode et al., 2019) we are beginning to move beyond model
569 species and investigate persistence in harvested and spatially-managed systems (e.g.,
570 Garavelli et al., 2018). Our study shows the importance of long term sampling and
571 careful consideration of the different demographic processes that affect our metric
572 calculations, such as density-dependence and sampling biases, to understand marine
573 population dynamics in empirical systems.

Figures

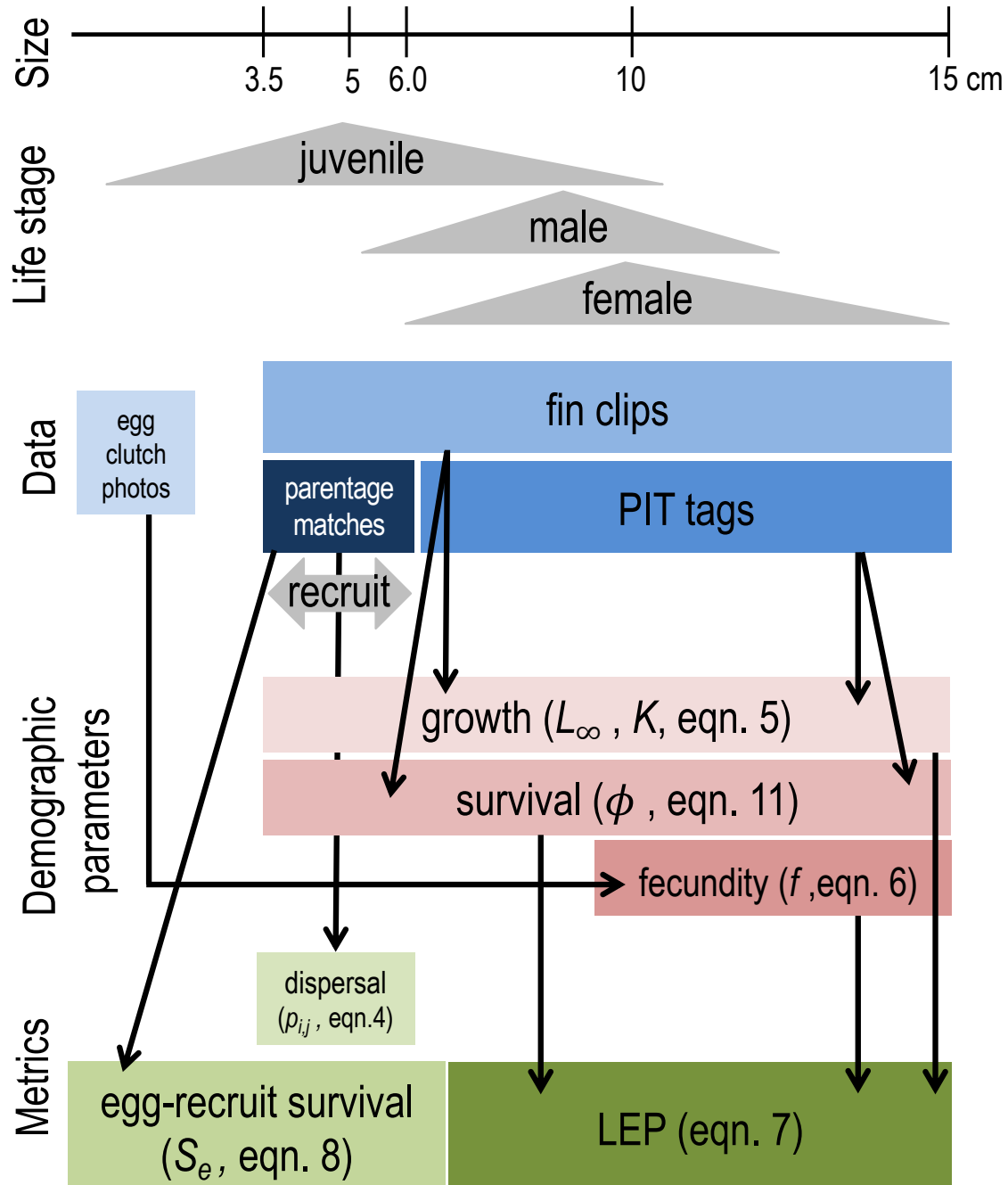


Figure 1: The data collected for fish at each life stage and how they match to the equations and metrics estimated. We consider recruits to be offspring in their first year of settlement, represented by the 3.5-6.0 cm range.

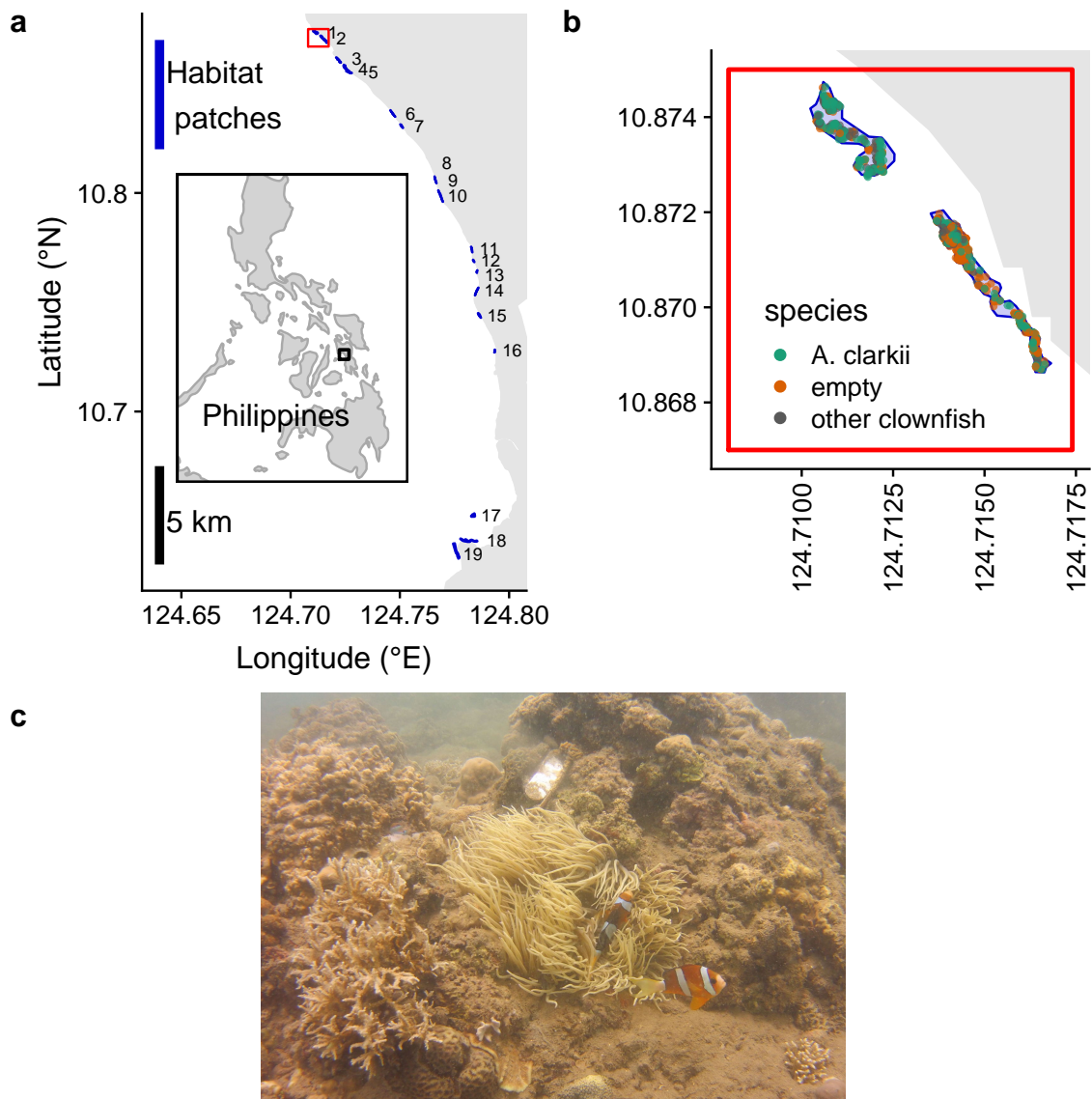


Figure 2: a) Map of the sites along the coast of Leyte in the Philippines. From north to south, the patches are: 1) Palanas, 2) Wangag, 3), North Magbangon, 4) South Magbangon, 5) Cabatoan, 6) Caridad Cemetery, 7) Caridad Proper, 8) Hicop South, 9) Sitio Tugas, 10) Elementary School, 11) Sitio Lonas, 12) San Agustin, 13) Poroc San Flower, 14) Poroc Rose, 15) Visca, 16) Gabas, 17) Tomakin Dako, 18) Haina, and 19) Sitio Baybayon. b) Zoomed-in map of the two northern-most sites, Palanas and Wangag, to show anemone arrangement with anemones colored as occupied by *A. clarkii* (green), occupied by other clownfish species (orange), or unoccupied by clownfish (grey). c) An example anemone occupied by *A. clarkii* in a typical habitat at the sites. The metal anemone tag is visible just above the anemone on the rock.

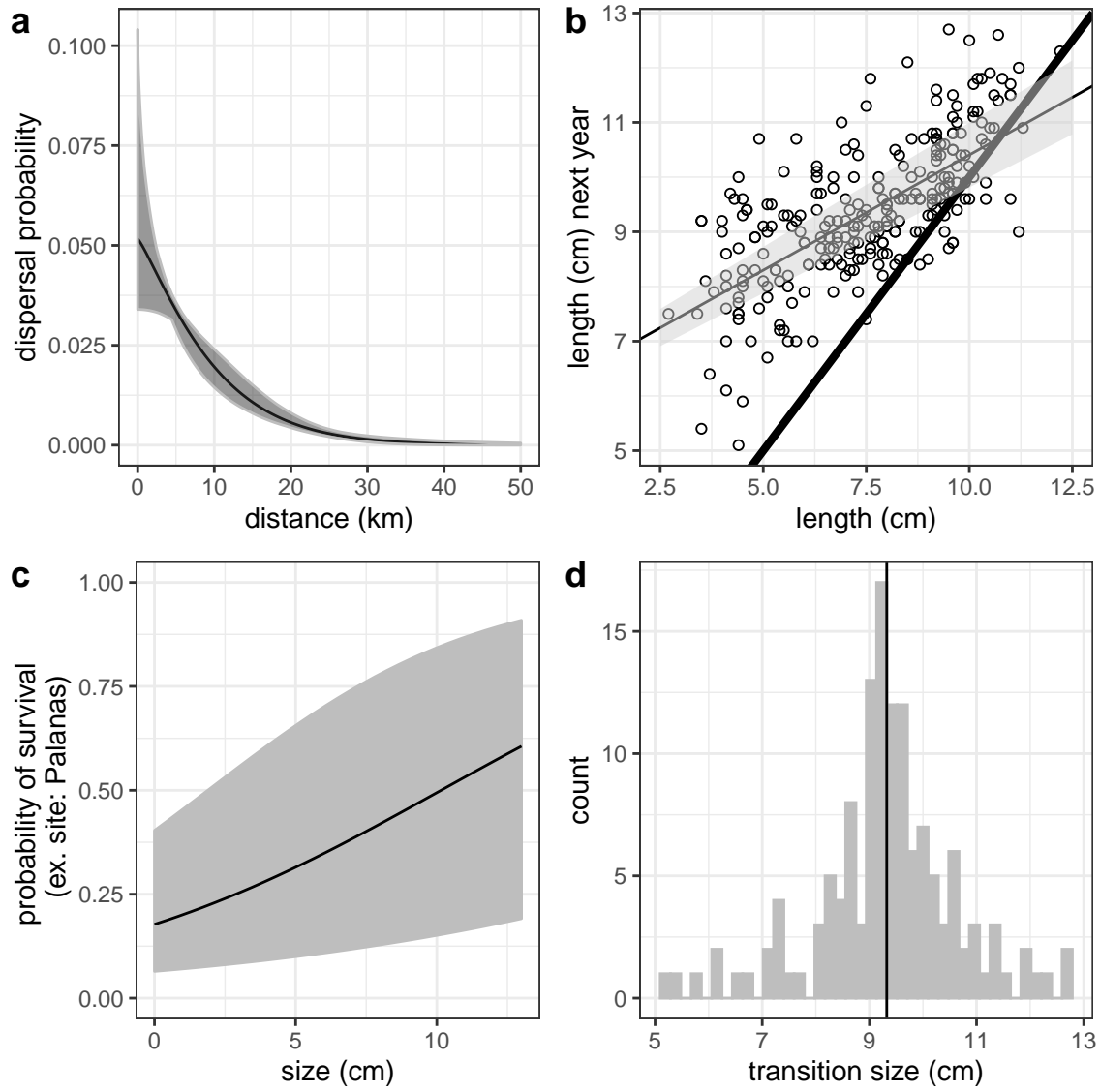


Figure 3: Best estimates (solid black line) and uncertainty (grey) for dispersal (a), growth, including the 1:1 line in thick black (b), post-recruit annual survival at Palanas as an example site (c), and size at female transition (d) parameters. Best est

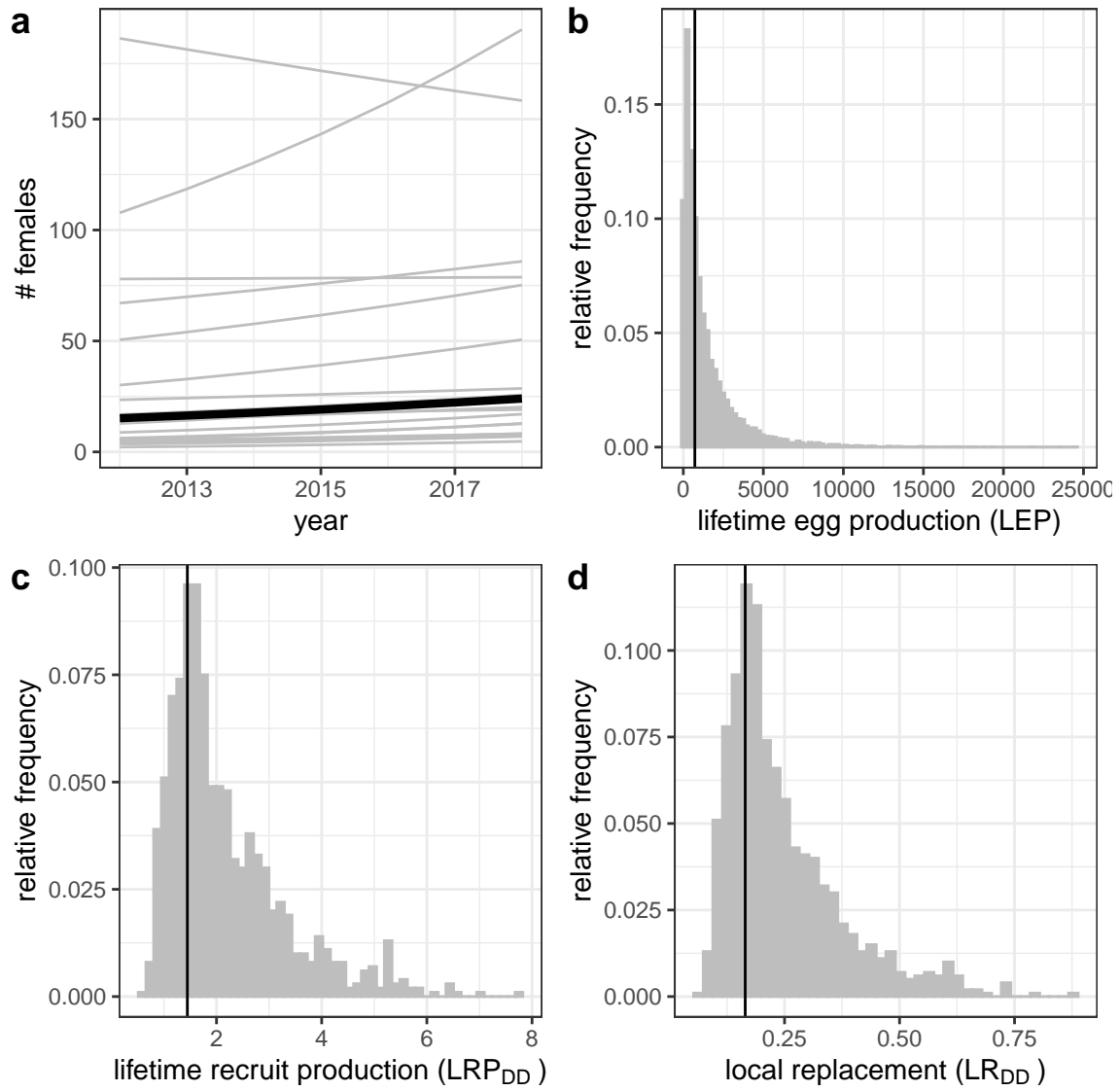


Figure 4: Estimates of a) estimated abundance of females over time at each individual site (grey lines) and for an average site (black line), b) individual-site LEP for all sites with the best estimate averaged across sites (black line), c) average LR_{DD} across sites, and d) local replacement, showing the best estimate (black solid line) and range of estimates considering uncertainty in the inputs (grey). Estimates of LRP and local replacement include compensation for density-dependent mortality in early life stages.

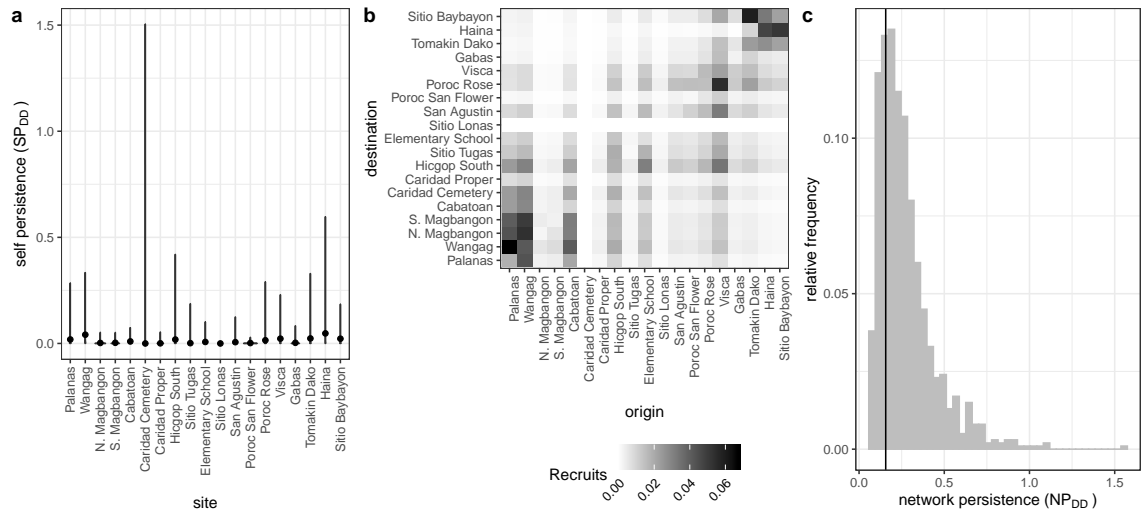


Figure 5: Values of self-persistence (a), realized connectivity among sites (b), and network persistence (c). All estimates include compensation for density-dependence in early life stages. For self-persistence (a) and network persistence (c), the best estimate is shown with in black (point for (a), line for (c)) and the range of estimates considering uncertainty is shown in grey.

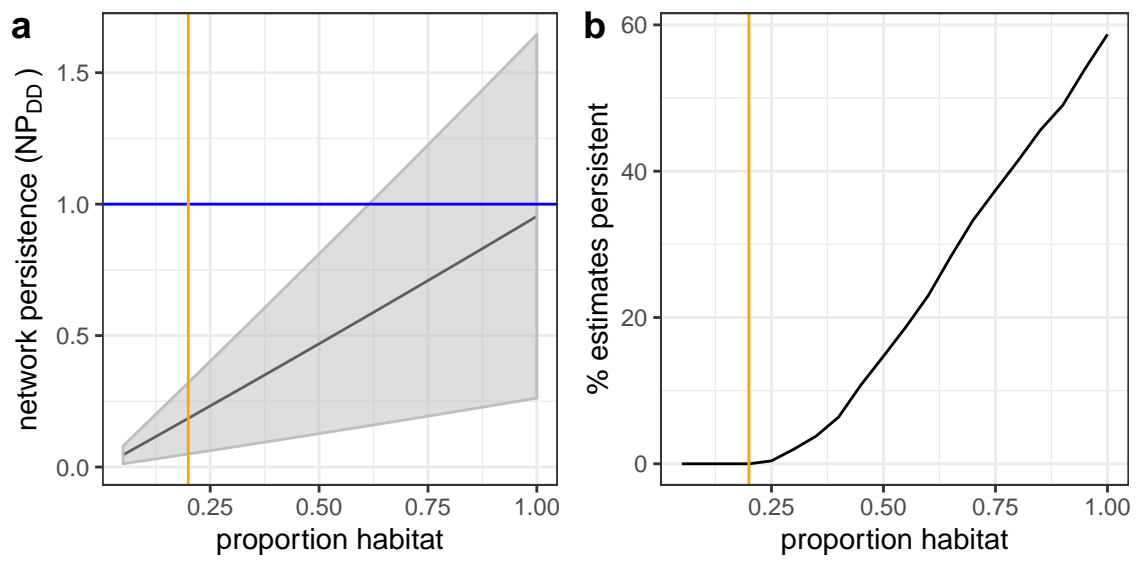


Figure 6: Sensitivity of network persistence to the proportion of the sampling region that is habitat. (a) The best estimate of λ_{cDD} with the standard deviation of the estimates with uncertainty for 19 patches of equal size and spacing with adult survivals for an average patch. (b) The percentage of estimates from the runs in (a) with $\lambda_{cDD} \geq 1$ with increasing proportion habitat.

Appendix

⁵⁷⁶ A Summary of parameters

| Parameter | Description | Best estimate | Range in uncertainty runs | Notes |
|------------|--|---------------|---------------------------|--|
| k_d | scale parameter in dispersal kernel | -2.33 | -2.81 to -1.22 | eqn. 4, estimated using methods in Bode et al. (2018) in Catalano et al. (in prep) |
| θ | shape parameter in dispersal kernel | 1.19 | 0.63 to 2.04 | eqn. 4, estimated using methods in Bode et al. (2018) in Catalano et al. (in prep) |
| L_∞ | average asymptotic size (cm) in von Bertalanffy growth curve | 10.70 cm | 9.81 to 11.65 cm | eqn. 5 |
| K | growth coefficient in von Bertalanffy growth curve | 0.864 | 0.80 to 0.91 | eqn. 5 |

| | | | | |
|--------------------------------|---|--------|---------------------------|-------------------------------|
| $b_{\phi_{Cabatoan}}$ | intercept for adult survival at 0 cm at Cabatoan | -1.78 | ± 0.33 standard error | on a log-odds scale, eqn. B.5 |
| $i_{\phi_{Cardidad Cemetery}}$ | addition to intercept for survival at Caridad Cemetery | -19.61 | ± 2994 standard error | on a log-odds scale, eqn. B.5 |
| $i_{\phi_{Elementary School}}$ | addition to intercept for survival at Elementary School | -0.11 | ± 0.41 standard error | on a log-odds scale, eqn. B.5 |
| $i_{\phi_{Gabas}}$ | addition to intercept for survival at Gabas | -0.42 | ± 0.58 standard error | on a log-odds scale, eqn. B.5 |
| $i_{\phi_{Haina}}$ | addition to intercept for survival at Haina | 0.12 | ± 0.35 standard error | on a log-odds scale, eqn. B.5 |
| $i_{\phi_{Hicgop South}}$ | addition to intercept for survival at Hicgop South | -0.06 | ± 0.46 standard error | on a log-odds scale, eqn. B.5 |

| | | | | |
|-----------------------------|--|-------|---------------------------|-------------------------------|
| $i_{\phi_{N.Magbangon}}$ | addition to intercept for survival at N. Magbangon | -1.31 | \pm 0.38 standard error | on a log-odds scale, eqn. B.5 |
| $i_{\phi_{Palanas}}$ | addition to intercept for survival at Palanas | 0.24 | \pm 0.26 standard error | on a log-odds scale, eqn. B.5 |
| $i_{\phi_{PorocRose}}$ | addition to intercept for survival at Poroc Rose | -0.19 | \pm 0.44 standard error | on a log-odds scale, eqn. B.5 |
| $i_{\phi_{PorocSanFlower}}$ | addition to intercept for survival at Poroc San Flower | -0.52 | \pm 0.48 standard error | on a log-odds scale, eqn. B.5 |
| $i_{\phi_{SanAgustin}}$ | addition to intercept for survival at San Agustin | -0.47 | \pm 0.50 standard error | on a log-odds scale, eqn. B.5 |
| $i_{\phi_{SitioBaybayon}}$ | addition to intercept for survival at Sitio Baybayon | 0.02 | \pm 0.26 standard error | on a log-odds scale, eqn. B.5 |

| | | | | |
|--------------------------|--|--------|---------------------------|------------------------------------|
| $i_{\phi_{S.Magbangon}}$ | addition to intercept for survival at S. Magbangon | -1.08 | \pm 0.48 standard error | on a log-odds scale, eqn. B.5 |
| $i_{\phi_{TomakinDako}}$ | addition to intercept for survival at Tomakin Dako | 0.39 | \pm 0.33 standard error | on a log-odds scale, eqn. B.5 |
| $i_{\phi_{Visca}}$ | addition to intercept for survival at Visca | 0.33 | \pm 0.35 standard error | on a log-odds scale, eqn. B.5 |
| $i_{\phi_{Wangag}}$ | addition to intercept for survival at Wangag | 0.35 | \pm 0.25 standard error | on a log-odds scale, eqn. B.5 |
| b_a | size effect for adult survival | 0.15 | \pm 0.03 standard error | on a log-odds scale, eqn. B.5 |
| β_e | coefficient for eyed eggs | -0.608 | | eqn. 6, Yawdoszyn et al. (in prep) |
| β_l | size effect in eggs-per-clutch relationship | 2.39 | | eqn. 6, Yawdoszyn et al. (in prep) |

| | | | | |
|-----------------------------------|---|---|--------------|--|
| b | intercept in eggs-per-clutch relationship at female size 0 cm | 1.17 | | eqn. 6, Yawdoszyn et al. (in prep) |
| c_e | egg clutches per year | 11.9 | | eqn. 6, Holtswarth et al. (2017) |
| $\text{size}_{\text{recruit}}$ | size (cm) of recruited offspring | mean of size of offspring in parentage analysis = 4.37 cm | 3.5 - 6.0 cm | drawn from uniform distribution across range |
| $\text{size}_{\text{recruit},sd}$ | standard deviation of size of a recruit | 0.1 | | used in discretization of IPM for LEP |
| size_{sd} | standard deviation distribution of sizes of a fish in the next year | 1.45 | | used in discretization of IPM for LEP, estimated from range of sizes for fish starting at 7.4-7.6 cm and recaptured a year later |

| | | | | |
|-------|--|--------------|---------------|--------------------------------------|
| L_s | minimum size in LEP IPM | 0 cm | | eqn. 7 |
| U_s | maximum size in LEP IPM | 15 cm | | eqn. 7 |
| L_f | size at transition to female | 9.32 cm | 5.2 - 12.7 cm | drawn from distribu- tion in data |
| R_m | number of off- spring matched to parents | 62 offspring | | eqn. 8 |
| N_g | number of geno- typed parents | 1719 fish | | eqn. 8 |
| P_h | proportion of sites sampled cumulatively across time | 0.41 | | eqn. 8, details in B.1 |
| P_d | proportion of dispersal kernel area from each site covered by our sampling region | 0.28 | | eqn. 8, details in B.3.0.1 |

| | | | | |
|-------|--|------|---|----------------------------|
| P_c | probability of capturing a fish | 0.56 | drawn from beta distribution with parameters $\alpha_{P_c} = 1.44$ and $\beta_{P_c} = 1.13$ | eqn. 8, details in B.2 |
| P_s | proportion of our sampling region that is habitat | 0.20 | | eqn. 8, details in B.3.0.2 |
| DD | proportion of habitat that would be available without density-dependence at settlement | 1.71 | | eqn. 8 |
| p_U | proportion of anemones unoccupied by clownfish | 0.53 | | used to estimate DD |

| | | | | |
|-------|--|------|--|---------------------|
| p_A | proportion of anemones occupied by $A.$ <i>clarkii</i> | 0.38 | | used to estimate DD |
|-------|--|------|--|---------------------|

Table A1: Summary of parameter symbols, definitions, and values.

B Method details

B.1 Proportion of habitat sampled

We used tagged anemones to estimate the proportion of habitat sampled at each site in each year ($P_{h_{i,t}}$). We tagged each anemone that is home to $A.$ *clarkii*, with a metal tag, which is relatively permanent and easy to re-sight (the anemone tag is visible above the anemone in Fig. 2c), so we consider the total number of metal tags at each site to be the total number of anemones that are habitat. We divide the number of tagged anemones visited each sampling year by the total number of metal tags at that site to get the proportion of habitat sampled. We use proportion of anemones rather than proportion of total site area because anemones, and therefore habitat quality, are unevenly distributed across the site; areas we did not visit are likely to have a lower density of anemones than the areas we did sample.

For scaling the number of tagged recruited offspring to account for areas of our sites we did not sample, we use the overall proportion habitat sampled across all sites and sampling years (P_h). We sum the metal-tagged anemones we visited across all

| Site | # Total anems | % Habitat surveyed | | | | | | |
|-------------------|---------------|--------------------|------|------|------|------|------|------|
| | | 2012 | 2013 | 2014 | 2015 | 2016 | 2017 | 2018 |
| Cabatoan | 26 | 42 | 58 | 58 | 65 | 73 | 0 | 62 |
| Caridad Cemetery | 4 | 0 | 75 | 50 | 0 | 50 | 50 | 50 |
| Elementary School | 8 | 0 | 100 | 38 | 88 | 88 | 88 | 100 |
| Gabas | 9 | 0 | 0 | 0 | 44 | 44 | 67 | 0 |
| Haina | 104 | 0 | 6 | 13 | 13 | 10 | 56 | 80 |
| Hicgop South | 18 | 0 | 67 | 22 | 28 | 56 | 83 | 78 |
| N. Magbangon | 105 | 5 | 12 | 40 | 63 | 63 | 0 | 5 |
| S. Magbangon | 34 | 41 | 56 | 32 | 0 | 65 | 0 | 71 |
| Palanas | 137 | 29 | 58 | 47 | 63 | 85 | 86 | 86 |
| Poroc Rose | 13 | 100 | 100 | 69 | 31 | 23 | 69 | 69 |
| Poroc San Flower | 11 | 100 | 82 | 73 | 73 | 55 | 82 | 64 |
| San Agustin | 17 | 94 | 65 | 71 | 65 | 100 | 82 | 76 |
| Sitio Baybaon | 260 | 0 | 14 | 30 | 33 | 30 | 41 | 80 |
| Tomakin Dako | 50 | 0 | 24 | 22 | 36 | 34 | 60 | 68 |
| Visca | 13 | 100 | 100 | 23 | 38 | 62 | 85 | 62 |
| Wangag | 296 | 18 | 32 | 42 | 34 | 26 | 49 | 68 |

Table A2: Table showing the percent of metal-tagged anemones surveyed at each site in each sampling year.

sites and years to get the total number of metal-tagged anemones we visited while sampling. We then divide that by the number of anemones we could have sampled,

594 the sum of total metal-tagged anemones across all sites multiplied by the number of sampling years, to get the overall proportion habitat sampled across our sites and sampling years.

597 **B.2 Probability of capturing a fish, from recapture dives**

We use mark-recapture data from recapture dives done within a sampling season to estimate the probability of capturing a fish. During some of the sampling years, portions of the sites were sampled again within a few weeks of the original sampling dives. We assume there is no mortality of tagged fish between the original sampling dives and the recapture dives because they are so close in time and that fish do not change their behavior or response to divers, so therefore assume that the probability of recapturing a fish is the same as the probability of capturing a fish on a sampling dive. For each recapture dive, we use GPS tracks of the divers to identify the anemones covered in the recapture dive and the set of PIT-tagged fish encountered on those anemones during the original sampling dives. We estimate the probability of capture P_c as the number of tagged fish caught during the capture dive m_2 divided by the total number of fish caught on the recapture dive n_2 : $P_c = \frac{m_2}{n_2}$. The value of P_c from each recapture dive is reported in Table A3.

We use the mean P_c across all 14 recapture dives, covering XX sites in 3 sampling seasons (2016, 2017, 2018), as our best estimate. Because there are so few recapture dives compared to the number of times we calculate the metrics to show the range of uncertainty, we represent the probability of capture as a distribution, rather than sampling directly from the values calculated for each recapture dive. The distribution of capture probabilities across the 14 dives is quite skewed so we represent it as a beta distribution, using the mean μ_{P_c} and variance V_{P_c} of the set of 14 values to find the appropriate α_{P_c} and β_{P_c} parameters, where

$$\alpha_{P_c} = \left(\frac{1 - \mu_{P_c}}{V_{P_c}} - \frac{1}{\mu_{P_c}} \right) \mu_{P_c}^2 \quad (\text{B.1})$$

$$\beta_{P_c} = \alpha_{\mu_{P_c}} \times \frac{1}{\mu_{P_c} - 1}. \quad (\text{B.2})$$

The mean of the individual capture probability values is $\mu_{P_c} = 0.56$, with variance $V_{P_c} = 0.069$, which gives beta distribution parameters $\alpha_{P_c} = 1.44$ and $\beta_{P_c} = 1.13$. We
 621 sample 1000 values from the beta distribution, then truncate the sample to only values larger than the lowest value of P_c estimated in an individual dive (0.20), to avoid extremely low values that are sometimes randomly sampled from the distribution
 624 but are unrealistically low. We then sample with replacement from the truncated set to get a vector of values the length of the number of runs.

Talk to Katrina to fill out table with data that went into recapture calcs

| Site | Year | m_2 | n_2 | P_c |
|------|------|-------|-------|-------|
| | | | | 0.56 |
| | | | | 0.26 |
| | | | | 0.89 |
| | | | | 0.67 |
| | | | | 0.20 |
| | | | | 0.83 |
| | | | | 0.47 |
| | | | | 0.20 |
| | | | | 0.83 |
| | | | | 1.0 |
| | | | | 0.33 |
| | | | | 0.58 |
| | | | | 0.63 |
| | | | | 0.41 |

Table A3: Table showing the site, year, number of fish caught on sample dives on the anemones resampled during the recapture dive (m_2), number of fish caught on the recapture dive (n_2) for each recapture dive.

⁶²⁷ B.3 Scaling up recruits

To estimate the total number of offspring produced by our genotyped parents that survive to recruitment, we scale up the number of matched offspring caught during sampling (R_m) to account for recruits we could have missed (Fig. B.1). We scale up by 1) the cumulative proportion of habitat we sampled at our sites over time (P_h) to account for recruits at anemones we did not sample (details in B.1), 2) the probability of capturing a fish if we sampled its anemone (P_c) to account for fish that escaped during sampling (details in B.2), 3) the proportion of the dispersal kernel from our sites within of our sampling region (P_d) to account for fish that dispersed outside of our sampling area (details in B.3.0.1), and 4) the proportion habitat in our

sampling region (P_s) to avoid counting mortality of fish dispersing to non-habitat within our region twice (in both the estimate of total recruits and in the integrated dispersal kernel) (details in B.3.0.2), and 5) the proportion of anemones occupied by *A. clarkii* (DD) to account for density-dependent mortality of settling recruits.

How could we have missed potential recruits originating from our sites?

- 1) Failed to catch recruit when sampling (P_c)
- 2) Missed sampling some habitat areas within our sites (P_h)
- 3) Recruit dispersed outside our study region (P_d)
- 4) Recruit dispersed to non-habitat within our region (P_s)
- 5) Recruit died due to density-dependent competition with other settlers (DD)

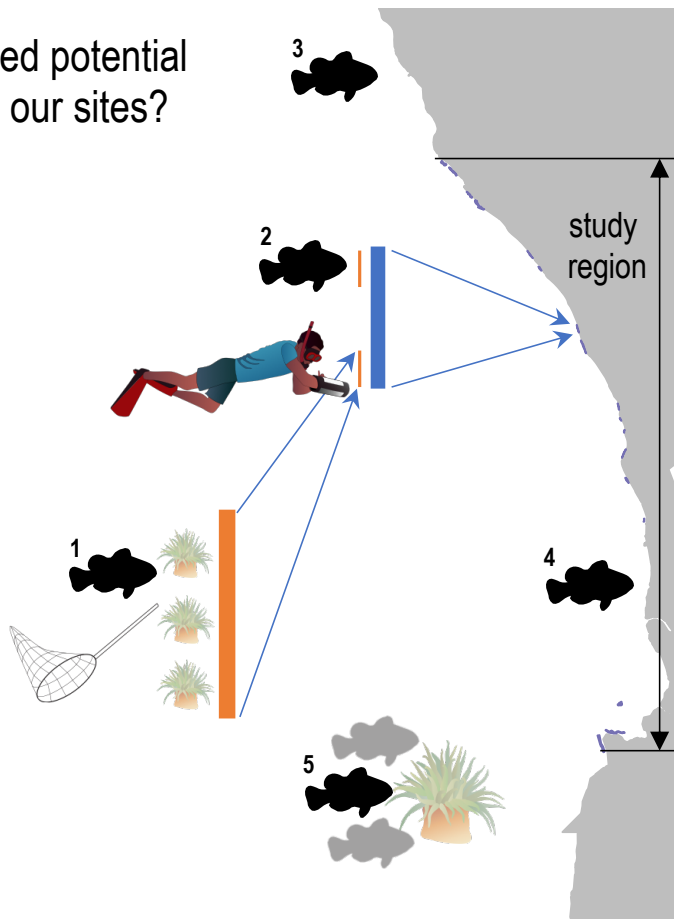


Figure B.1: Schematic of five ways we could have missed recruits while sampling and used to scale up our raw estimate of recruits from matched offspring.

B.3.0.1 Proportion of dispersal kernel area sampled

642 To account for recruits that dispersed outside our sampling region, we find the proportion of the dispersal kernels from all parents that falls within our sampling region.
 For each of the nineteen sites, we find the area (A_i) under the kernel from the center of the site to the north edge of the sampling area (d_N) (northern-most tagged
 645 anemone at Palanas, the northern-most site) and the center of the site to the south edge of the sampling area (d_S) (southern-most tagged anemone at Sitio Baybayon,
 648 the southern-most site), then multiply by the number of genotyped parents at that site (N_{g_i}). We add the total areas together, then divide by the sum of the total area under the dispersal kernel in both directions (1 when kernel is normalized to 0.5)
 651 multiplied by the total number of genotyped parents (N_g) to get the proportion of the total dispersal kernel area covered by our sampling region (P_d):

$$A_i(d) = N_{g_i} \int_0^{d_N} z e^{-(zd)^{\theta}} dd, \quad (\text{B.3})$$

$$P_d = \frac{\sum_{i=1}^{19} A_i}{N_g}. \quad (\text{B.4})$$

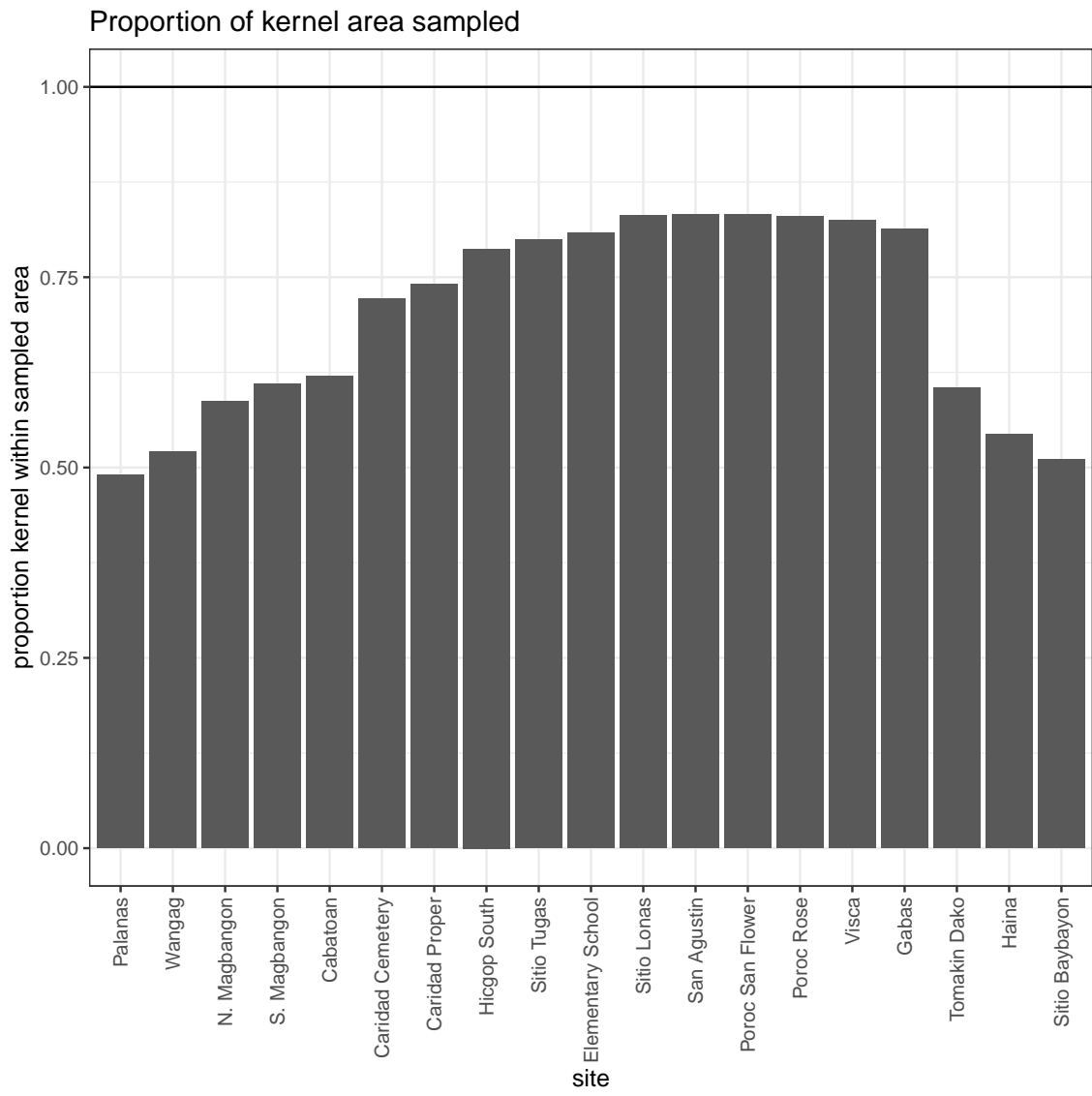


Figure B.2: Proportion of the dispersal kernel area from the center of each site covered by our sampling. Our overall proportion is weighted by the number of parents at each site.

B.3.0.2 Proportion habitat in sampling area

We assume that larvae are unable to navigate to habitat if they attempt to settle on an unsuitable patch, though clownfish larvae do likely have some ability both to sense good settlement areas, either by detecting host anemones (Elliott et al., 1995; Arvedlund et al., 1999) or conspecifics (e.g. Lecchini et al., 2005, for coral reef fish more broadly), and swim in particular direction (e.g. Bellwood and Fisher, 2001; Fisher, 2005). To avoid counting mortality due to settling on non-habitat twice - once in scaling up our matched recruits, which only includes those who settled on habitat, and once in integrating the dispersal kernel, we scale our estimate of total surviving recruits from our patches by the proportion of our sampling region that is habitat (P_s). We find P_s by summing the lengths of all of our sites, which run approximately north-south, and dividing that by the total distance north-south of our sampling region, giving $P_s = 0.20$.

| Model | Model description | AICc | dAICc |
|-----------------------------|--|----------|-----------|
| $\phi \sim S, p \sim S + D$ | survival size, recapture size+distance | 3348.861 | 0 |
| $\phi \sim S, p \sim D$ | survival size, recapture distance | 3359.998 | -11.1371 |
| $\phi, p \sim D$ | survival constant, recapture distance | 3383.175 | 34.3141 |
| $\phi, p \sim S + D$ | survival constant, recapture size+distance | 3384.959 | 36.0981 |
| $\phi \sim t, p$ | survival time, recapture constant | 3408.342 | 59.4816 |
| $\phi \sim i, p$ | survival site, recapture constant | 3440.842 | 91.98112 |
| $\phi \sim i, p \sim S + D$ | survival site, recapture size+distance | 3440.842 | 91.98112 |
| $\phi, p \sim t$ | survival constant, recapture time | 3453.609 | 104.74839 |
| $\phi \sim S, p \sim S$ | survival size, recapture size | 3527.710 | 178.84940 |
| ϕ, p | survival constant, recapture constant | 3570.908 | 222.04690 |

Table A4

666 B.4 Full set of MARK models

We consider the following set of models in MARK for survival (ϕ) and recapture (p) probability, including effects of size (S), minimum distance from diver to anemone 669 during surveys (D), time (t), and site (i) (Table A4):

The best model for post-recruitment annual survival ϕ has a positive size effect 672 ($b_a = 0.169 \pm 0.028$ SE UPDATE THESE NUMBERS!) with intercepts varying by site (eqn. B.5, Fig. B.3). The best model for recapture probability p_r has a negative 675 effect of size ($b_1 = -1.816 \pm 0.080$ SE UPDATE THESE NUMBERS!) and a negative effect of diver distance from anemone ($b_2 = -0.171 \pm 0.021$ SE UPDATE THESE NUMBERS!), with intercept $b_{p_r} = 17.93 \pm 0.858$ SE UPDATE THESE NUMBERS! (eqn. B.6, Fig. B.4), suggesting divers are less likely to recapture larger fish and those

at anemones far from areas sampled.

$$\log\left(\frac{\phi}{1-\phi}\right) = b_{\phi_i} + b_a \text{size}. \quad (\text{B.5})$$

$$\log\left(\frac{p_r}{1-p_r}\right) = b_{p_r} + b_1 \text{size} + b_2 d. \quad (\text{B.6})$$

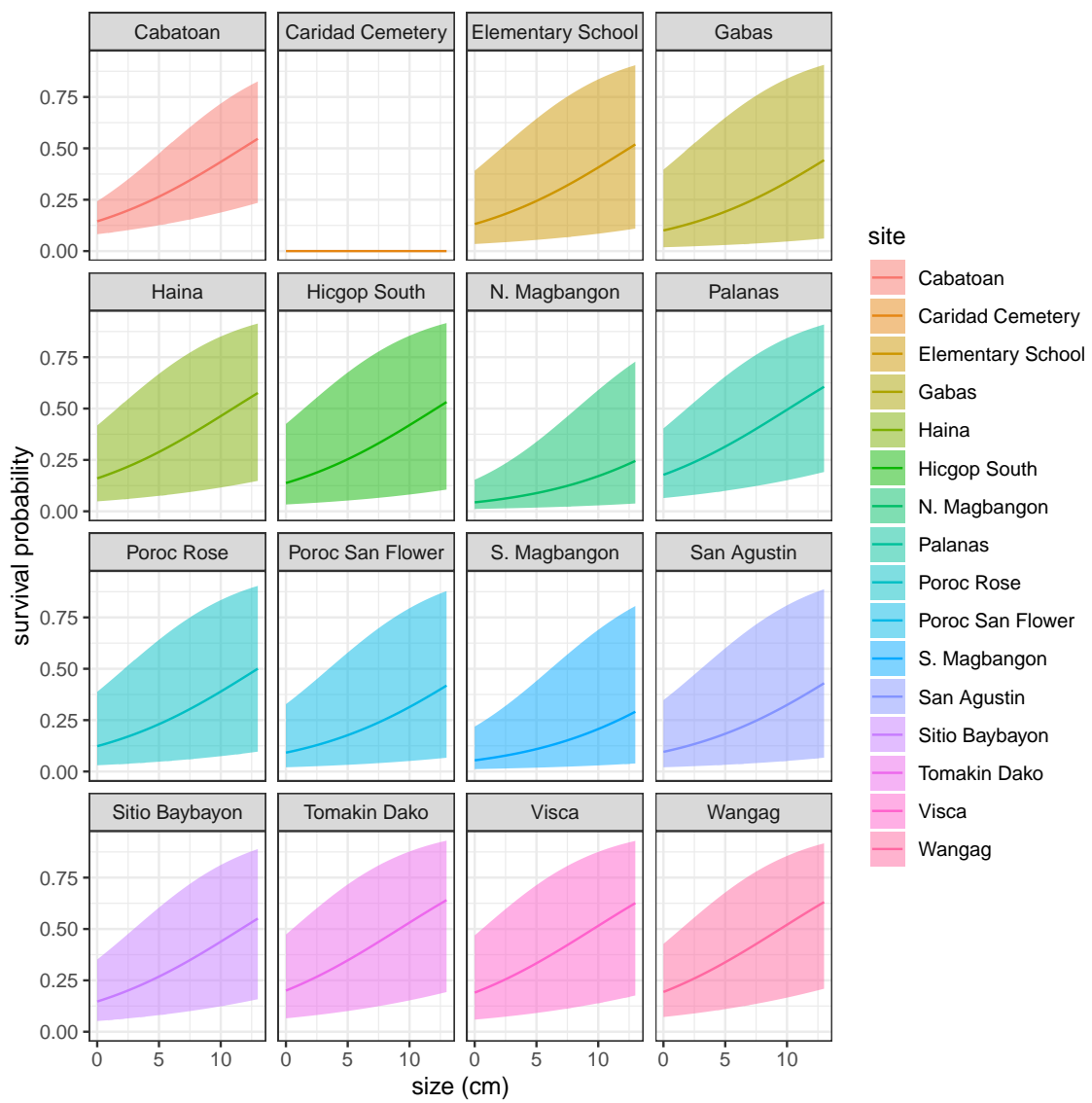


Figure B.3: Annual survival by size at each site.

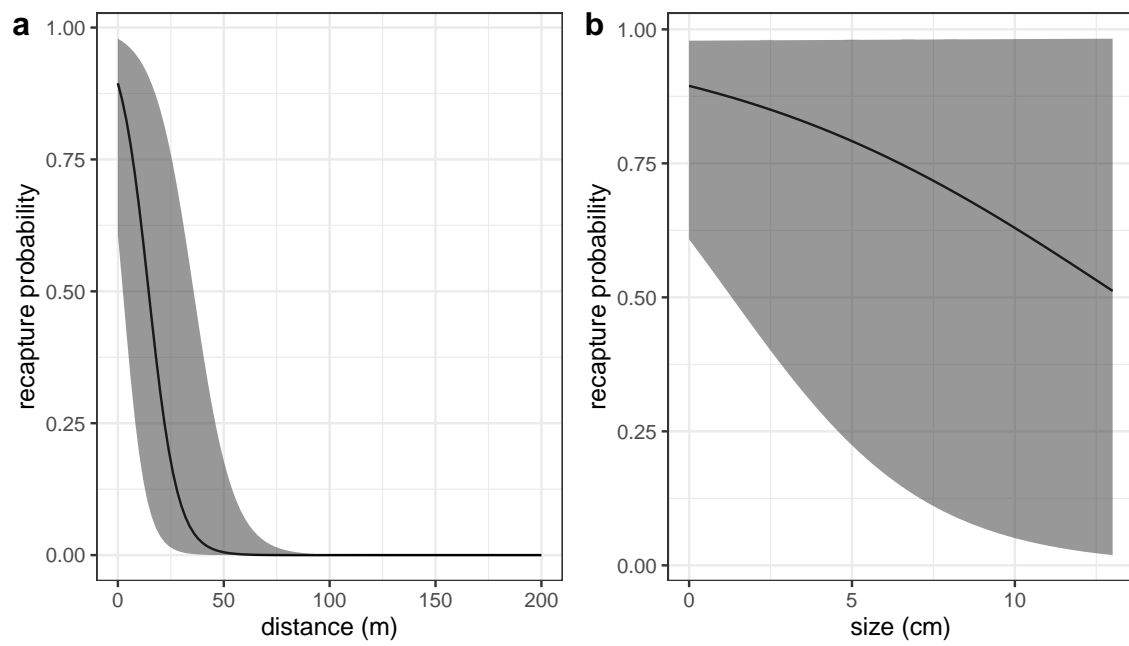


Figure B.4: Effects of a) minimum distance between divers and the anemone where the fish was first caught and b) fish size on the probability the fish will be recaptured, estimated along with survival in a mark-recapture analysis. Size has a slightly negative effect on the probability of recapture - larger fish are stronger swimmers and more likely to flee the anemone when divers approach, but with high uncertainty at larger sizes. Distance also has a negative effect on recapture, as fish tend to stay close to their anemones and are not likely to be recaptured if divers do not get close to their anemone.

678 **C Result details and sensitivity**

C.1 Abundance trends by site

We use the number of females captured at each site in each sampling year, scaled by
681 the proportion of habitat sampled at that site in that year and by the probability of
capturing a fish, to estimate abundance trends for each site (Fig. C.1).

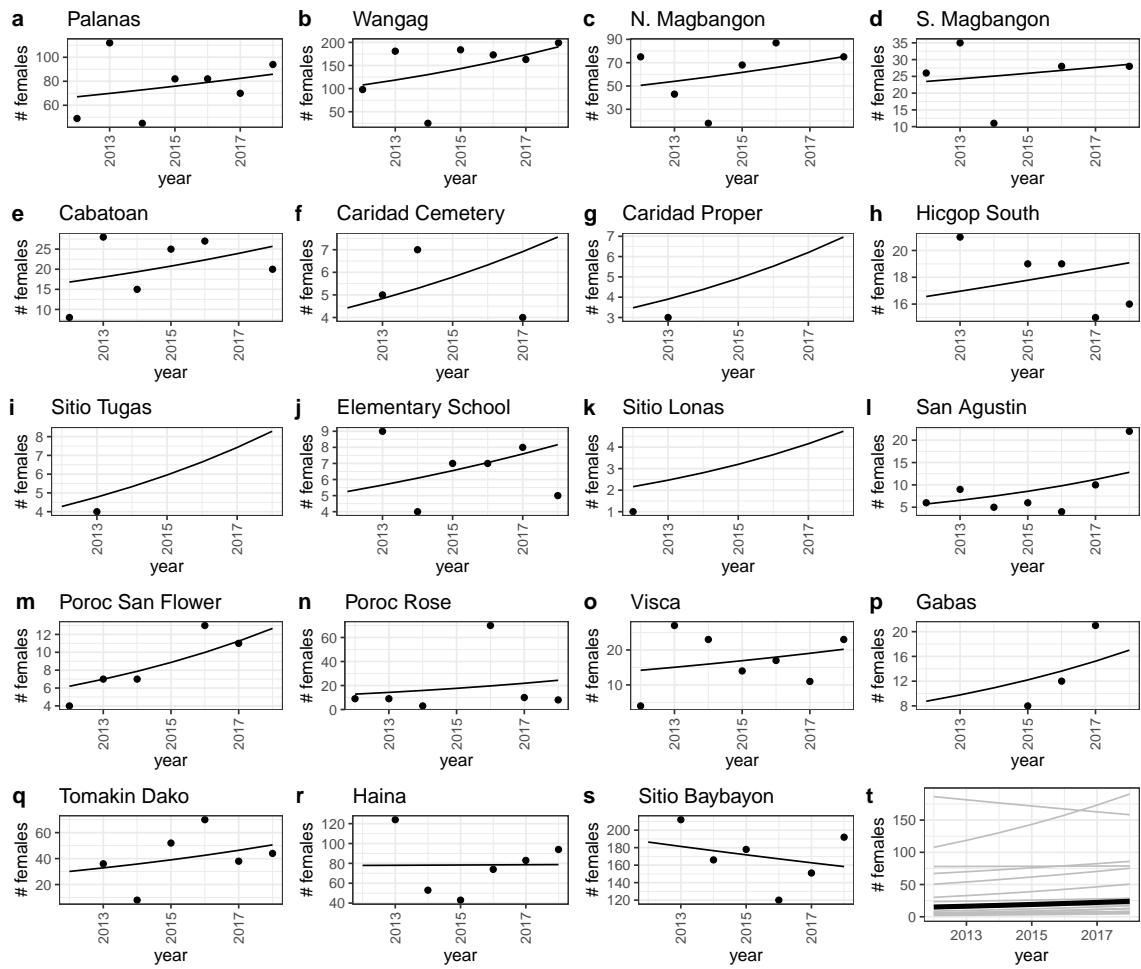


Figure C.1: Scaled number of females captured (black dots) and abundance trends (black lines) by site from a mixed effects model with site as a random effect.

C.2 Compensating for density dependence

684 Estimating persistence metrics without compensating for density-dependence in our
data gives us an understanding of whether individuals at our sites are able to replace
themselves and whether our sites persist as in isolation at the current abundance
687 levels, rather than at low abundance. Without compensation for early life density-
dependence, all of our metrics show that the set of sites we sample is less likely to
persist as an isolated network. We estimate egg-recruit survival (S_e) to be 7.8e-04
690 [1.2e-04, 0.033] and average lifetime recruit production (LRP) across sites to be 0.83
[0.28, 3.89], with XX% of LRP estimates ≥ 1 . (Fig. C.2c). Our estimate of local
replacement (LR), which estimates replacement for recruits from our sites returning
693 to our sites implicitly including dispersal, is 0.09 [0.03, 0.44].

When we calculate LR using all arriving recruits to our sites, however, rather
than just those originating there, the best estimate is > 1 (1.22, with XX% of values
696 with uncertainty ± 1), suggesting that there is recruit-recruit replacement at our sites
when we include immigrant recruits.

We do not find any sites with a best estimate or uncertainty range of $SP > 1$
699 (Figs. C.3a), with the exception of the wide uncertainty bounds on SP for Caridad
Cemetery. Our best estimate of the dominant eigenvalue of the realized connectivity
matrix λ_c is 0.21 [0.07, 0.92] with $p(\lambda \geq 1 = XX)$ (Fig. C.3c).

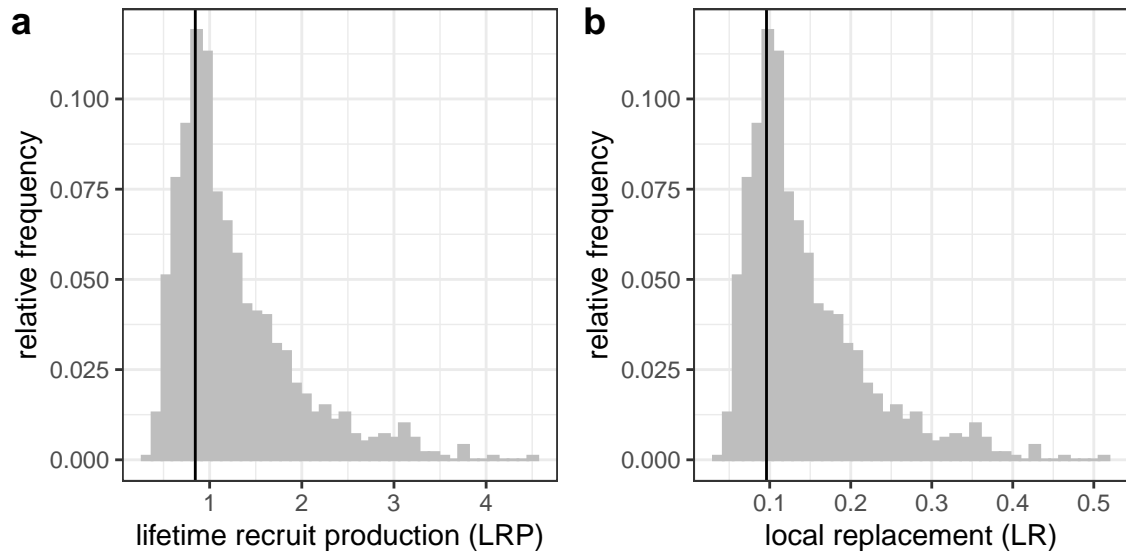


Figure C.2: Estimates of a) LRP, and b) local replacement without compensating for density dependence in early life stages in our data, showing the best estimate (black solid line) and range of estimates considering uncertainty in the inputs. These estimates compare to those in 4c,d, where we correct for additional mortality in early life due to density dependence.

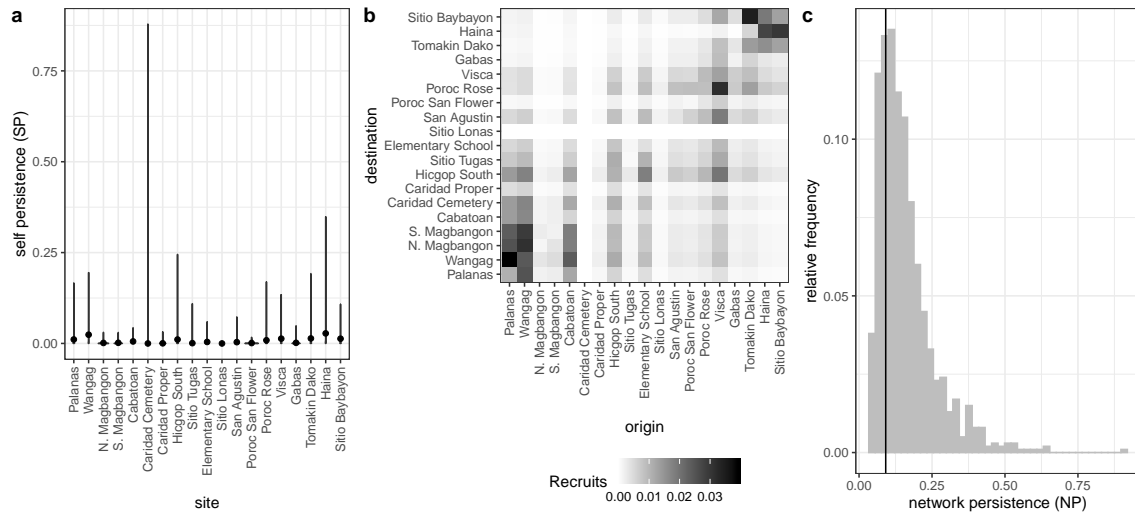


Figure C.3: Values of self-persistence (a), realized connectivity among sites (b), and network persistence (c) without compensation for density-dependence in early life stages in our data. For self-persistence (a) and network persistence (c), the best estimate is shown with in black (point for (a), line for (c)) and the range of estimates considering uncertainty is shown in grey. These estimates compare to those in 5 where we attempt to compensate for density dependence in early life stages.

⁷⁰² C.3 LEP and LRP by site

WRITE SOME TEXT!

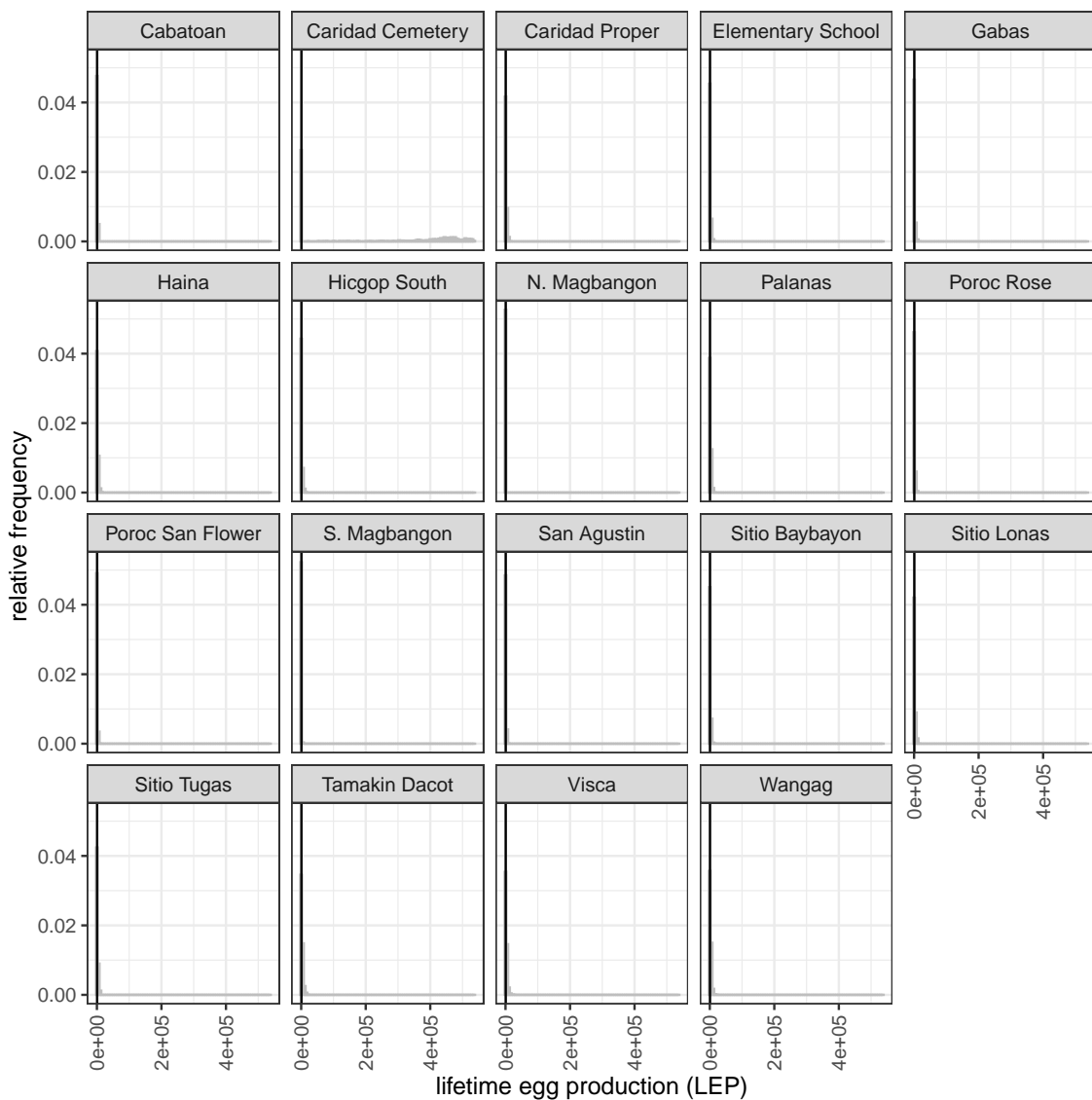


Figure C.4: Write a caption.

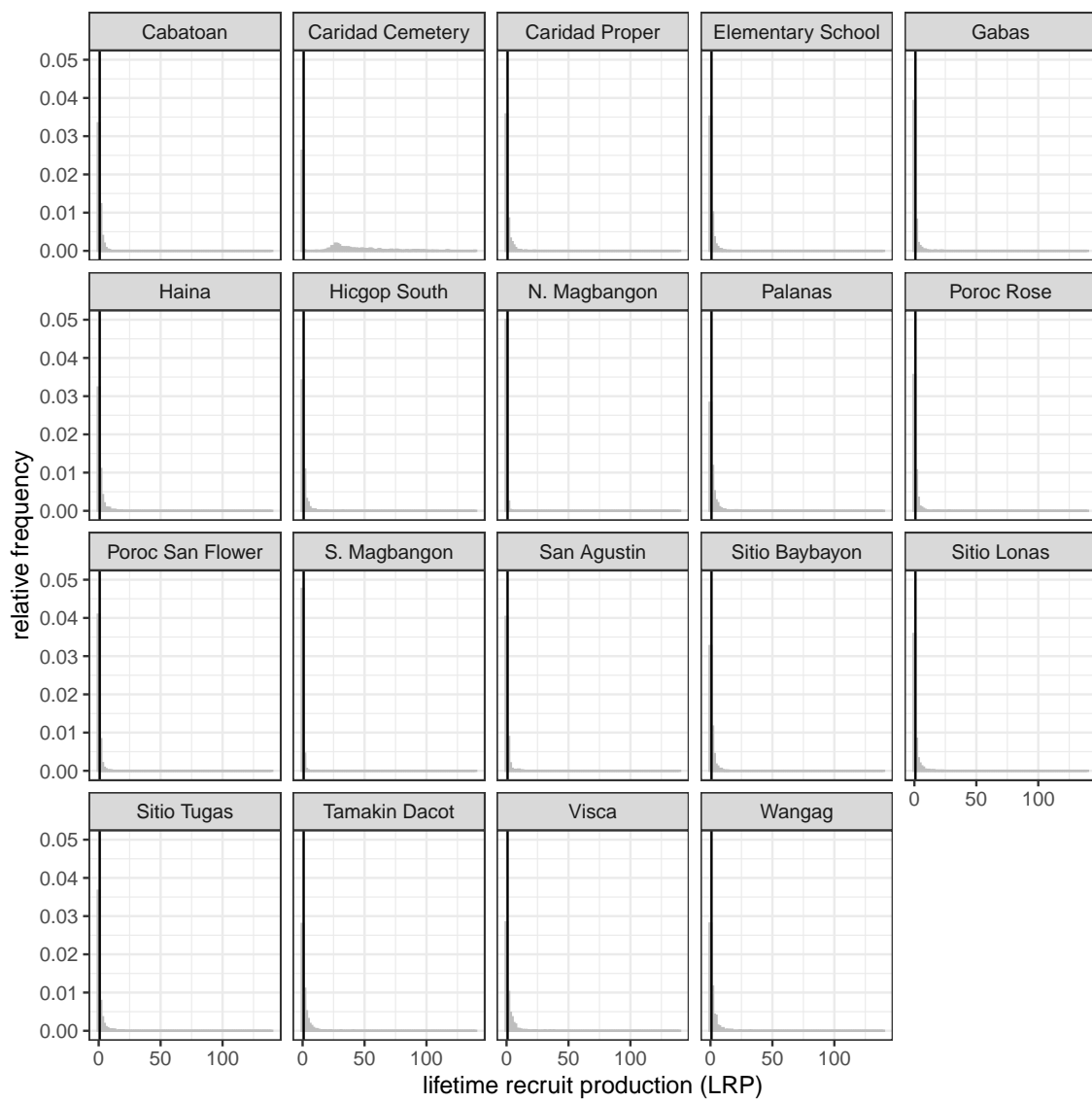


Figure C.5: Write a caption.

C.4 Sensitivity to parameters

⁷⁰⁵ The range of parameters not shown in the main text (Fig. 3):

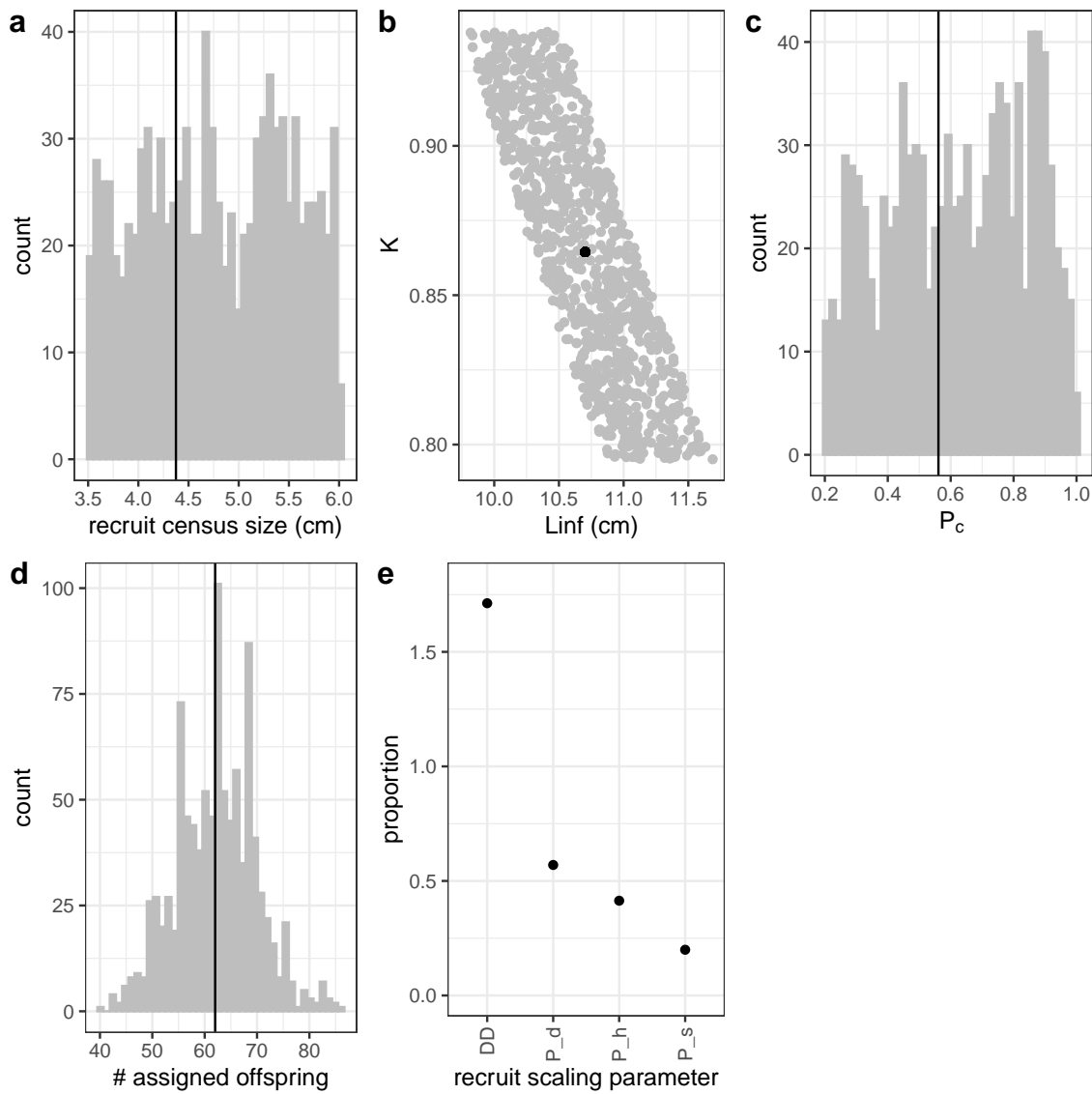


Figure C.6: Range of parameter inputs for uncertainty runs with all uncertainty included, where the black line or point is the value used for the best estimate: a) $\text{size}_{\text{recruit}}$, the census size at which fish are considered to have recruited after egg-recruit survival occurs; b) the parameters L_{∞} and K of the von Bertalanffy growth model; c) P_c , the probability of capturing a fish; d) number of offspring assigned back to parents in the parentage analysis; e) factors that scale the number of estimated recruits from our site based on density-dependence in settler success (DD), proportion of the dispersal kernel captured by our sampling region (P_d), the cumulative proportion of our sites we sampled over time (P_h), and the proportion of our sampling area that is habitat (P_s).

C.5 Effects of different types of uncertainty on metrics

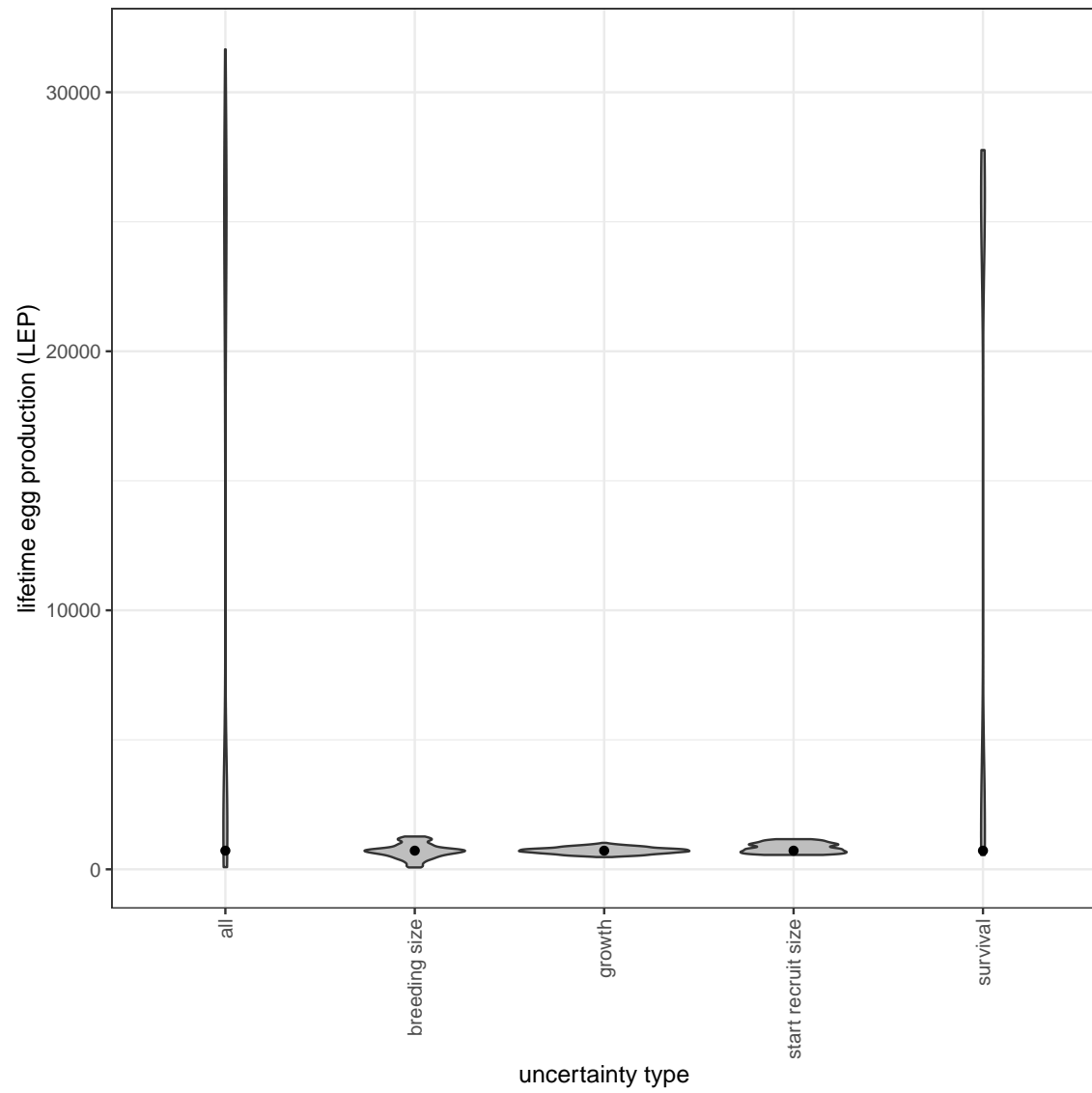


Figure C.7: The contribution of different sources of uncertainty in LEP.

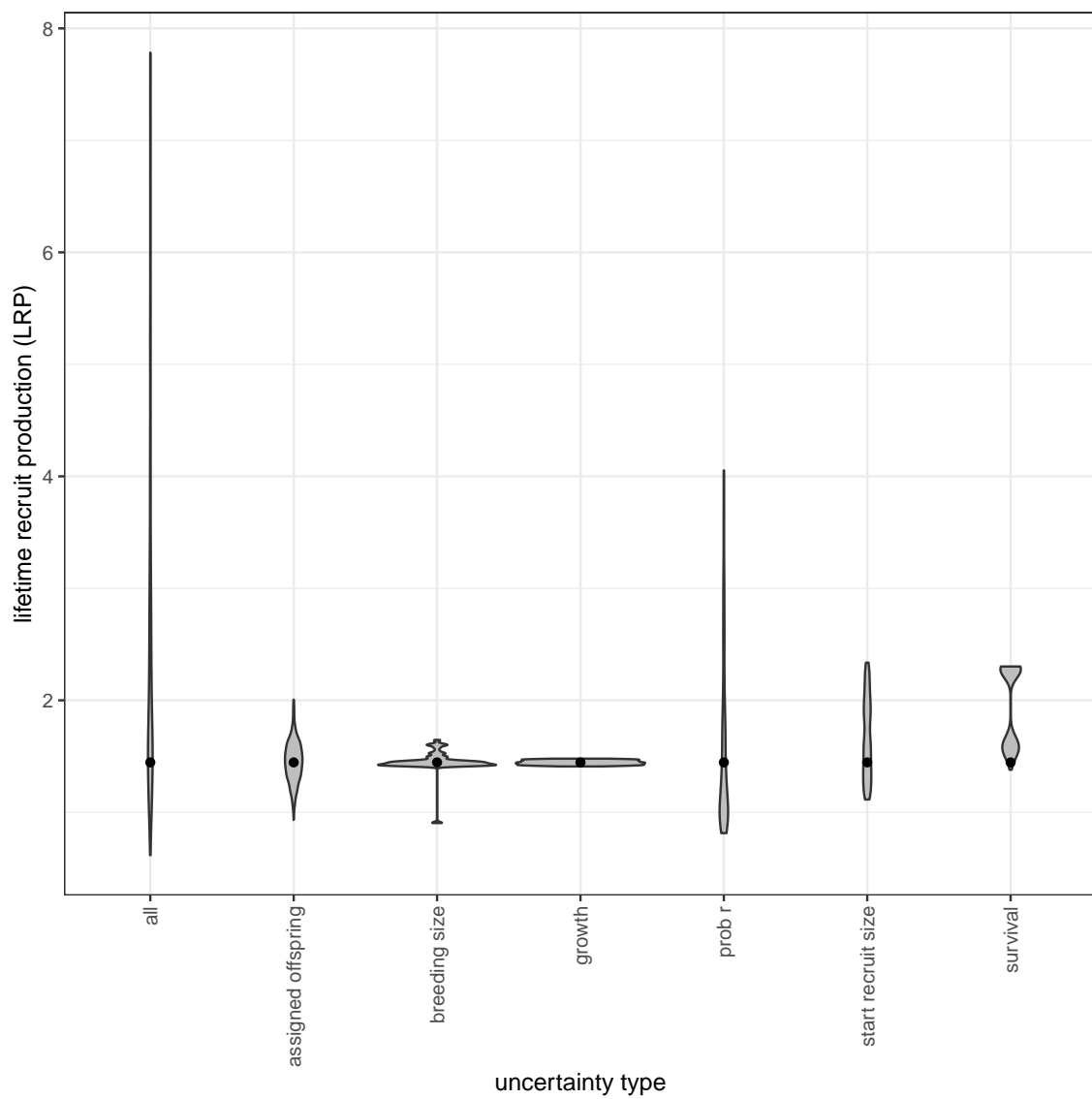


Figure C.8: The contribution of different sources of uncertainty in LRP.

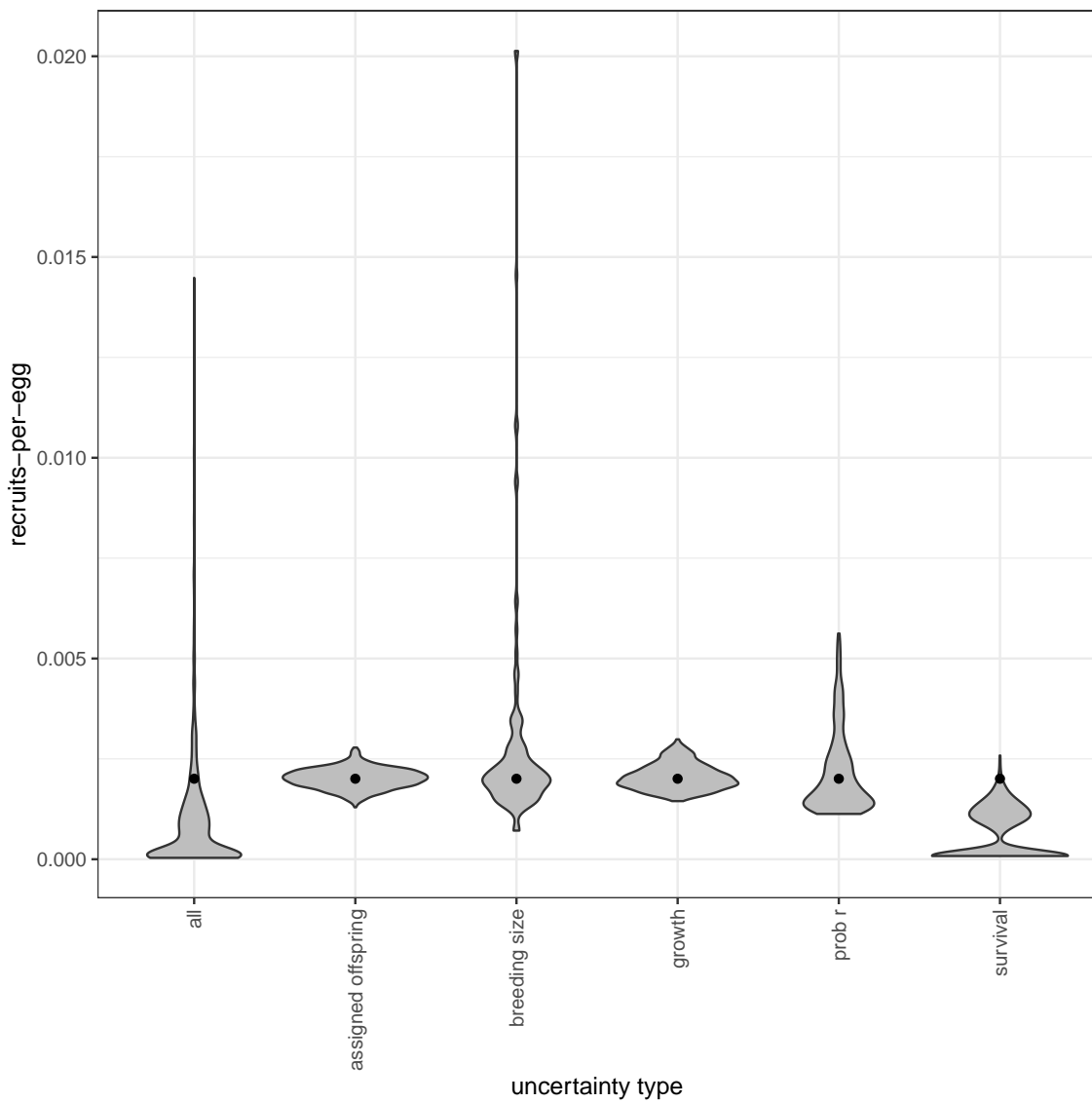


Figure C.9: The contribution of different sources of uncertainty in egg-recruit survival.

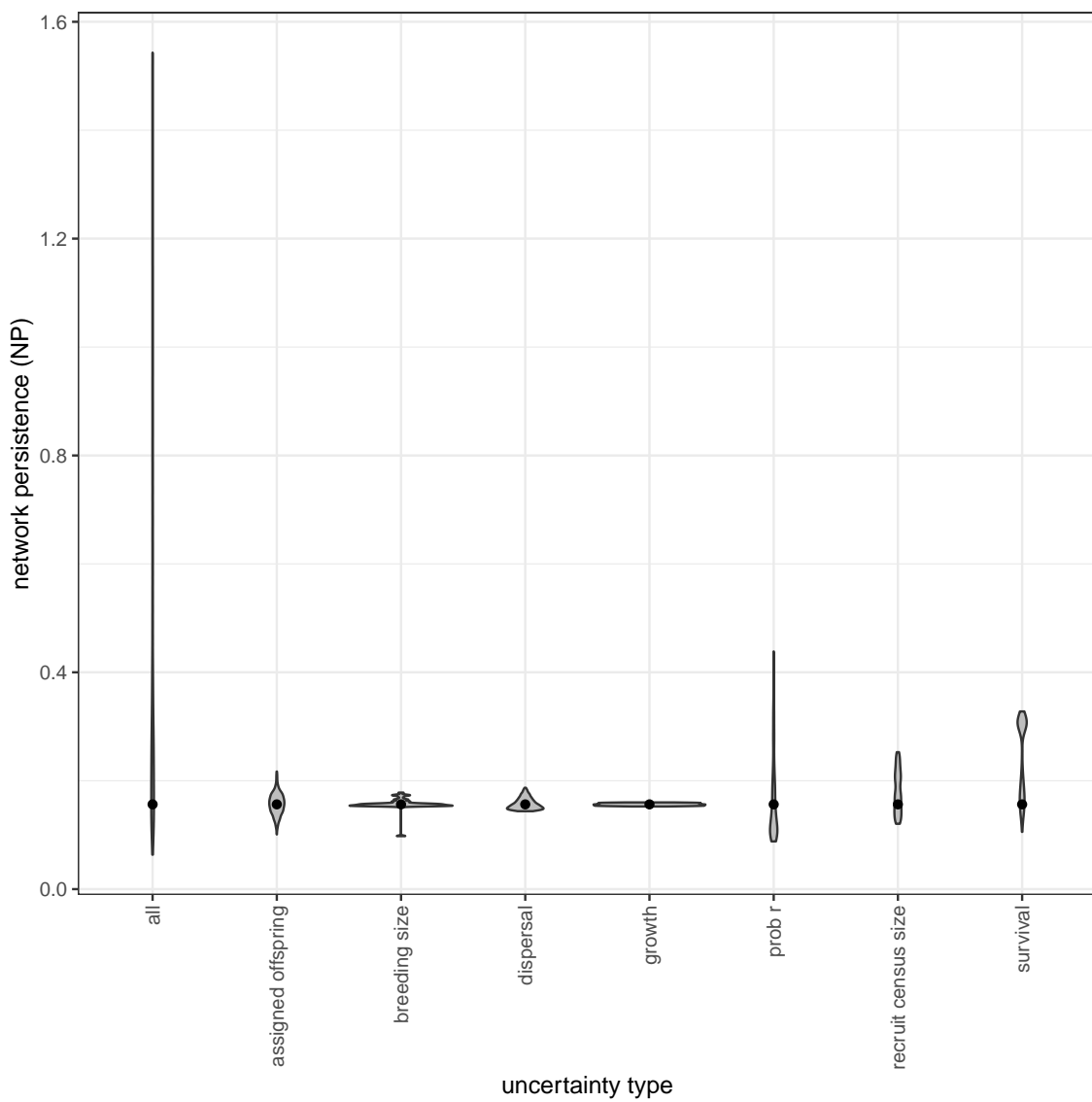


Figure C.10: The contribution of different sources of uncertainty in NP.

References

- 708 Glenn R Almany, Serge Planes, Simon R Thorrold, Michael L Berumen, Michael
Bode, Pablo Saenz-Agudelo, Mary C Bonin, Ashley J Frisch, Hugo B Harrison,
Vanessa Messmer, et al. Larval fish dispersal in a coral-reef seascape. *Nature
Ecology & Evolution*, 1:0148, 2017.
- 711 Michael Arvedlund, Mark I McCormick, Daphne G Fautin, and Mogens Bildsøe. Host
recognition and possible imprinting in the anemonefish *amphiprion melanopus*
714 (pisces: Pomacentridae). *Marine Ecology Progress Series*, 188:207–218, 1999.
- 717 Diana S Baetscher, Eric C Anderson, Elizabeth A Gilbert-Horvath, Daniel P Malone,
Emily T Saarman, Mark H Carr, and John Carlos Garza. Dispersal of a nearshore
marine fish connects marine reserves and adjacent fished areas along an open coast.
Molecular ecology, 28(7):1611–1623, 2019.
- 720 Douglas Bates, Martin Mächler, Ben Bolker, and Steve Walker. Fitting linear mixed-
effects models using lme4. *Journal of Statistical Software*, 67(1):1–48, 2015. doi:
10.18637/jss.v067.i01.
- 723 David R Bellwood and Rebecca Fisher. Relative swimming speeds in reef fish larvae.
Marine Ecology Progress Series, 211:299–303, 2001.
- 726 Michael Bode, David H Williamson, Hugo B Harrison, Nick Outram, and Geoffrey P
Jones. Estimating dispersal kernels using genetic parentage data. *Methods in
Ecology and Evolution*, 9(3):490–501, 2018.

- Michael Bode, Jeffrey M. Leis, Luciano B. Mason, David H. Williamson, Hugo B. Harrison, Severine Choukroun, and Geoffrey P. Jones. Successful validation of a
729 larval dispersal model using genetic parentage data. *PLOS Biology*, 17(7):1–13,
07 2019. doi: 10.1371/journal.pbio.3000380. URL <https://doi.org/10.1371/journal.pbio.3000380>.
- Louis W. Botsford, Alan Hastings, and Steven D. Gaines. Dependence of sustainability on the configuration of marine reserves and larval dispersal distance. *Ecology Letters*, 4:144–150, 2001.
732
- Louis W Botsford, J Wilson White, and Alan Hastings. *Population Dynamics for Conservation*. Oxford University Press, 2019.
735
- Scott C Burgess, Kerry J Nickols, Chris D Griesemer, Lewis AK Barnett, Allison G Dedrick, Erin V Satterthwaite, Lauren Yamane, Steven G Morgan, J Wilson White, and Louis W Botsford. Beyond connectivity: how empirical methods can quantify population persistence to improve marine protected-area design. *Ecological Applications*, 24(2):257–270, 2014.
738
741
- Peter Buston. Forcible eviction and prevention of recruitment in the clown anemonefish. *Behavioral Ecology*, 14(4):576–582, 2003a.
- Peter Buston. Social hierarchies: size and growth modification in clownfish. *Nature*,
744 424(6945):145–146, 2003b.
- Peter M Buston and Cassidy C DAloia. Marine ecology: reaping the benefits of local
747 dispersal. *Current Biology*, 23(9):R351–R353, 2013.

Peter M Buston and Jane Elith. Determinants of reproductive success in dominant pairs of clownfish: a boosted regression tree analysis. *Journal of Animal Ecology*,
750 80(3):528–538, 2011.

Peter M Buston, Geoffrey P Jones, Serge Planes, and Simon R Thorrold. Probability
of successful larval dispersal declines fivefold over 1 km in a coral reef fish. *Pro-
753 ceedings of the Royal Society of London B: Biological Sciences*, page rspb20112041,
2011.

Henry S Carson, Geoffrey S Cook, Paola C López-Duarte, and Lisa A Levin. Eval-
756 uating the importance of demographic connectivity in a marine metapopulation.
Ecology, 92(10):1972–1984, 2011.

Hal Caswell. *Matrix population models: construction, analysis, and interpretation*.
759 Sinauer Associates Inc., Sunderland, Massachusetts, 2nd edition, 2001.

Katrina A Catalano, Allison G Dedrick, Michelle Stuart, Jonathan Purtiz, Humberto
Montes, Jr., and Malin Pinsky. Interannual variability of genetic connectivity in
762 a coral reef fish *Amphiprion clarkii*. in prep.

C. C. D'Aloia, S. M. Bogdanowicz, J. E. Majoris, R. G. Harrison, and P. M. Buston.
Self-recruitment in a Caribbean reef fish: a method for approximating dispersal
765 kernels accounting for seascape. *Molecular Ecology*, 22(9):2563–2572, May 2013.
ISSN 09621083. doi: 10.1111/mec.12274. URL <http://doi.wiley.com/10.1111/mec.12274>.

₇₆₈ Cassidy C DAloia, Steven M Bogdanowicz, Robin K Francis, John E Majoris, Richard G Harrison, and Peter M Buston. Patterns, causes, and consequences of marine larval dispersal. *Proceedings of the National Academy of Sciences*, 112
₇₇₁ (45):13940–13945, 2015.

₇₇₄ JK Elliott, JM Elliott, and RN Mariscal. Host selection, location, and association behaviors of anemonefishes in field settlement experiments. *Marine Biology*, 122 (3):377–389, 1995.

₇₇₇ Stephen P Ellner, Dylan Z Childs, Mark Rees, et al. Data-driven modelling of structured populations. *A practical guide to the Integral Projection Model*. Cham: Springer, 2016.

Augustus J. Fabens. Properties and fitting of the von bertalanffy growth curve. *Growth*, 29:265–289, 1965.

₇₈₀ Daphne Gail Fautin, Gerald R Allen, Gerald Robert Allen, Australia Naturalist, Gerald Robert Allen, and Australie Naturaliste. Field guide to anemonefishes and their host sea anemones. 1992.

₇₈₃ Will F Figueira. Connectivity or demography: defining sources and sinks in coral reef fish metapopulations. *Ecological Modelling*, 220(8):1126–1137, 2009.

₇₈₆ Rebecca Fisher. Swimming speeds of larval coral reef fishes: impacts on self-recruitment and dispersal. *Marine Ecology Progress Series*, 285:223–232, 2005.

Lysel Garavelli, J Wilson White, Iliana Chollett, and Laurent Marcel Chérubin. Population models reveal unexpected patterns of local persistence despite widespread larval dispersal in a highly exploited species. *Conservation Letters*, 11(5):e12567, 2018.

Sarah O Hameed, J Wilson White, Seth H Miller, Kerry J Nickols, and Steven G Morgan. Inverse approach to estimating larval dispersal reveals limited population connectivity along 700 km of wave-swept open coast. *Proceedings of the Royal Society B: Biological Sciences*, 283(1833):20160370, 2016.

Ilkka Hanski. Metapopulation dynamics. *Nature*, 396(6706):41–49, 1998.

Hugo B Harrison, David H Williamson, Richard D Evans, Glenn R Almany, Simon R Thorrold, Garry R Russ, Kevin A Feldheim, Lynne Van Herwerden, Serge Planes, Maya Srinivasan, et al. Larval export from marine reserves and the recruitment benefit for fish and fisheries. *Current biology*, 22(11):1023–1028, 2012.

Deborah R Hart and Antonie S Chute. Estimating von bertalanffy growth parameters from growth increment data using a linear mixed-effects model, with an application to the sea scallop *placopecten magellanicus*. *ICES Journal of Marine Science*, 66 (10):2165–2175, 2009.

Alan Hastings and Louis W. Botsford. Persistence of spatial populations depends on returning home. *Proceedings of the National Academy of Sciences*, 103:6067–6072, 2006.

- 807 Akihisa Hattori and Yasunobu Yanagisawa. Life-history pathways in relation to
gonadal sex differentiation in the anemonefish, *amphiprion clarkii*, in temperate
waters of japan. *Environmental Biology of Fishes*, 31(2):139–155, 1991.
- 810 Kina Hayashi, Katsunori Tachihara, and James Davis Reimer. Low density popu-
lations of anemonefish with low replenishment rates on a reef edge with anthro-
pogenic impacts. *Environmental Biology of Fishes*, 102(1):41–54, 2019.
- 813 Jordan N. Holtswarth, Shem B. San Jose, Humberto R. Montes Jr., James W. Morley,
and Malin. L Pinsky. The reproductive seasonality and fecundity of yellowtail
clownfish (*amphiprion clarkii*) off the philippines. *Bulletin of Marine Science*, 93,
816 2017.
- Darren W Johnson, Mark R Christie, Timothy J Pusack, Christopher D Stallings,
and Mark A Hixon. Integrating larval connectivity with local demography reveals
819 regional dynamics of a marine metapopulation. *Ecology*, 99(6):1419–1429, 2018.
- J.L. Laake. RMark: An r interface for analysis of capture-recapture data with
MARK. AFSC Processed Rep. 2013-01, Alaska Fish. Sci. Cent., NOAA,
822 Natl. Mar. Fish. Serv., Seattle, WA, 2013. URL [http://www.afsc.noaa.gov/
Publications/ProcRpt/PR2013-01.pdf](http://www.afsc.noaa.gov/Publications/ProcRpt/PR2013-01.pdf).
- David Lecchini, Serge Planes, and René Galzin. Experimental assessment of sensory
825 modalities of coral-reef fish larvae in the recognition of their settlement habitat.
Behavioral Ecology and Sociobiology, 58(1):18–26, 2005.

Dale R Lockwood, Alan Hastings, and Louis W Botsford. The effects of dispersal
828 patterns on marine reserves: does the tail wag the dog? *Theoretical population
biology*, 61(3):297–309, 2002.

Haruki Ochi. Mating behavior and sex change of the anemonefish, *amphiprion clarkii*,
831 in the temperate waters of southern japan. *Environmental Biology of Fishes*, 26
(4):257–275, 1989.

Malin L Pinsky, Humberto R Montes Jr, and Stephen R Palumbi. Using isolation
834 by distance and effective density to estimate dispersal scales in anemonefish. *Evo-
lution*, 64(9):2688–2700, 2010.

BJ Puckett and DB Eggleston. Metapopulation dynamics guide marine reserve de-
837 sign: importance of connectivity, demographics, and stock enhancement. *Eco-
sphere*, 7(6), 2016.

H Ronald Pulliam. Sources, sinks, and population regulation. *The American Natu-
ralist*, 132(5):652–661, 1988.
840

Océane C Salles, Glenn R Almany, Michael L Berumen, Geoffrey P Jones, Pablo
Saenz-Agudelo, Maya Srinivasan, Simon R Thorrold, Benoit Pujol, and Serge
843 Planes. Strong habitat and weak genetic effects shape the lifetime reproductive
success in a wild clownfish population. *Ecology letters*, 23(2):265–273, 2020.

Ocane C. Salles, Jeffrey A. Maynard, Marc Joannides, Corentin M. Barbu, Pablo
846 Saenz-Agudelo, Glenn R. Almany, Michael L. Berumen, Simon R. Thorrold, Ge-
offrey P. Jones, and Serge Planes. Coral reef fish populations can persist without

immigration. *Proceedings of the Royal Society B: Biological Sciences*, 282(1819):

849 20151311, November 2015. ISSN 0962-8452, 1471-2954. doi: 10.1098/rspb.2015.

1311. URL <http://rspb.royalsocietypublishing.org/lookup/doi/10.1098/rspb.2015.1311>.

852 Diane M Thompson, J Kleypas, F Castruccio, Enrique N Curchitser, Malin L Pinsky,
B Jönsson, and James R Watson. Variability in oceanographic barriers to coral
larval dispersal: Do currents shape biodiversity? *Progress in oceanography*, 165:
855 110–122, 2018.

Nick Tolimieri and Phillip S Levin. The roles of fishing and climate in the population
dynamics of bocaccio rockfish. *Ecological Applications*, 15(2):458–468, 2005.

858 Jinliang Wang. Sibship reconstruction from genetic data with typing errors. *Genetics*,
166(4):1963–1979, 2004.

Jinliang Wang. Estimation of migration rates from marker-based parentage analysis.
861 *Molecular ecology*, 23(13):3191–3213, 2014.

J. Wilson White, Mark H Carr, Jennifer E Caselle, Libe Washburn, C. Brock Wood-
son, Stephen R Palumbi, Peter M Carlson, Robert R Warner, Bruce A Menge,
864 John A Barth, Carol A Blanchette, Peter T Raimondi, and Kristen Milligan. Con-
nectivity, dispersal, and recruitment: Connecting benthic communities and the
coastal ocean. *Oceanography*, 32(3):50–59, 2019.

867 Jw White, Lw Botsford, A Hastings, and Jl Largier. Population persistence in ma-
rine reserve networks: incorporating spatial heterogeneities in larval dispersal.

Marine Ecology Progress Series, 398:49–67, January 2010. ISSN 0171-8630, 1616-

870 1599. doi: 10.3354/meps08327. URL <http://www.int-res.com/abstracts/meps/v398/p49-67/>.

Adam Yawdoszyn. Fecundity in clownfish. in prep.